MACH Rocketry Spring 2020 Report

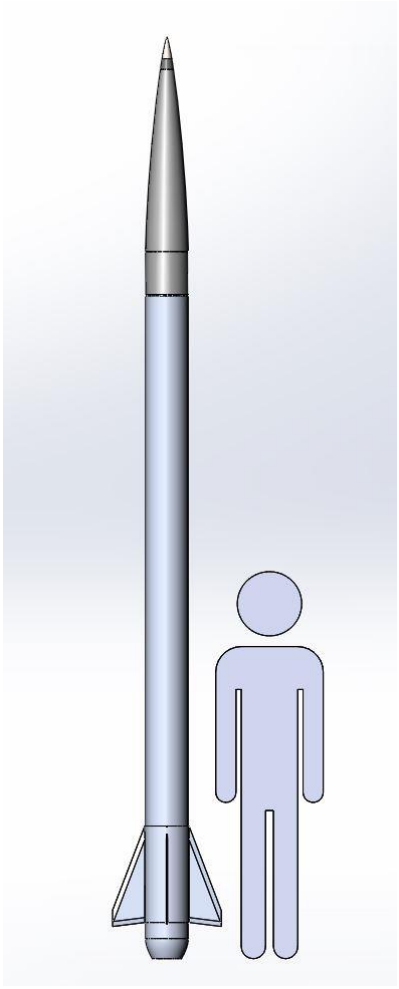

Luke Egbert, Team Lead

Jamie Weiss, Team Lead

Adam DeCino

TC Della Penna

Kian Roybal

Trevor Toft

Abstract

In Spring 2017, we launched our first rocket for this project. The first rockets were hobby store Estes kits and quickly after these first launches, we were launching our first high power rockets to obtain certifications that would allow us to fly larger, more powerful rockets. After 18 months of flying rockets and learning all we could, we began planning for our proof of concept rocket in late Spring 2019. This rocket was to be a data acquisition tool that would allow us to see how well our designs translated into the real world and how well our software predicted the flight. During the Summer 2019 we wrote a MATLAB code to predict the rocket flight which included supersonic airflow and coefficient of drag calculations well beyond Mach. The test rocket went to 35,300 ft and Mach 2.0 as predicted by the software. This flight also proved that our other designed components functioned as well; these included fins, ejection charges, motor closures, and the nozzle. After this success we were ready to move forward with the larger design and planning started in August 2019. This rocket was originally planned to reach Mach 4.5 at 30,000 ft and then proceed to an altitude of over 300,000 ft. Unfortunately, due to budgetary restrictions, we were forced to scale back the project and optimize the design for weight and speed. We took what we could from the rocket that we launched and began to redesign. The simulations said that the rocket would reach over 65,000 ft and Mach 3.0. At these speeds and altitudes special considerations must be made, including fin geometry/vibration, surface area reduction, rigid motor to air frame attachment, and high-altitude ejection charges. As we began design of these components we simultaneously designed and tested a new, more energetic propellant. We optimized the fins for the minimum surface area, minimum weight, and the highest possible Mach number without the fins vibrating apart. By weight reducing the coupling

mechanism we were able to reduce its weight by almost 50% over the previous design and still maintain rigidity. High-altitude ejection charges were tested in a custom built vacuum chamber with a pressure sensor and a variety of charges were tested so we could obtain the most desirable results. The launch date for this rocket has been pushed back due to unforeseen circumstances, but we do plan on flying it as soon as possible.

Table of Contents

List of Figures

Figure 48: Resulting volume of LV-Haack nose cone as solve by program.

List of Tables

Introduction

Rocketry is something that we have been doing since the beginning of 2017 and it is exciting now that we are working towards such a large goal with the biggest rocket we have ever built. Going through design and analysis has been very important since we started getting into higher power rockets with very large amounts of thrust. There are many factors that can affect a rockets flight from, drag, to atmospheric conditions, to stability of the rocket and so on. Taking these things into account into our simulation program that we designed will be very helpful in predicting our rocket's flight.

Getting the opportunity to launch our 4-inch sub-minimum diameter rocket at BALLS 28 was very important in determining what kind of design we were going to pursue forward with. Since the design worked so well, and the flight went excellent, we wanted to upscale the rocket, but due to budgetary restrictions, we had to scale the project back. The motor was also a very important aspect of that flight because we fully tested and characterized the propellant and launched the largest motor that we had ever mixed. Working on the propellant for so long has taught us a lot about the way it behaves and the way that we want to modify it for the final rocket. Machining the aluminum coupler between the motor casing and the payload was vital because we were able to do finite element analysis on it and knew that it would withstand the flight that it was going to undergo.

Analyzing not only the flight but the material selection has been very beneficial. We have tested three different kinds of materials that are used to make rockets and by a large margin filament wound fiberglass is the strongest and the one that we have been using, and will continue to use, for these high impulse flights. We wanted to wind our own fiberglass

and test those samples to see how they compare to the off the shelf fiberglass, but due to campus closing we were going to use off the shelf fiberglass instead.

A simulation method was developed to aid the rocketry design process. Routines have been programmed as needed to obtain mass properties for the distinct sections of a rocket. This MATLAB procedure will take in known geometries of the rocket and return their calculated mass values. Most notably, this software will work in reverse and take in an allowed mass as input and solve for an optimal nose cone thickness. This thickness is not arbitrary and will provide the cross-sectional area that satisfies the maximum allowable stress along with its safety factor. This procedure is tentative and to be developed and updated as the selected material mass-properties are researched.

Launch from BALLS 28

We attended BALLS 28 on the Black Rock Desert in Nevada from September 20-22, 2019. We prepared over the Summer and start of the Fall 2019 semester and launched a 4-inch sub-minimum diameter rocket on an experiment N3300 to an altitude of 35,300 feet and 1550 mph. The casing, fin can, fiberglass, and electronics were off the shelf, but the motor, electronics bay, and aluminum coupler were manufactured by the team. The motor was an 8 grain 98 mm made from the Purple Pig propellant and had about 3300 N of average thrust, 14,000 N-s of impulse, and a 3.7 second burn time. The length of the grains near the forward closure were shorter than the grains near the nozzle because of the high L/D of the motor. The grains were also stepped with a larger core near the nozzle to account for the erosive burning that would have happened if the grains were not stepped. Erosive burning happens when the diameter of the core of the grain is too close to the diameter of the nozzle

throat and the exhaust gases as they are ejected erodes the nozzle. The launch was very successful and allowed us to fly a similar model to what we are building for senior design.

Original and Modified Design

Design of the final rocket will be influenced heavily by testing that we have yet to conduct and data that we have collected from previous rocket launches. The summer project for the BALLS 28 launch gave a lot of good data and worked as a proof of concept for a scaled down version of the final rocket that we plan to launch.

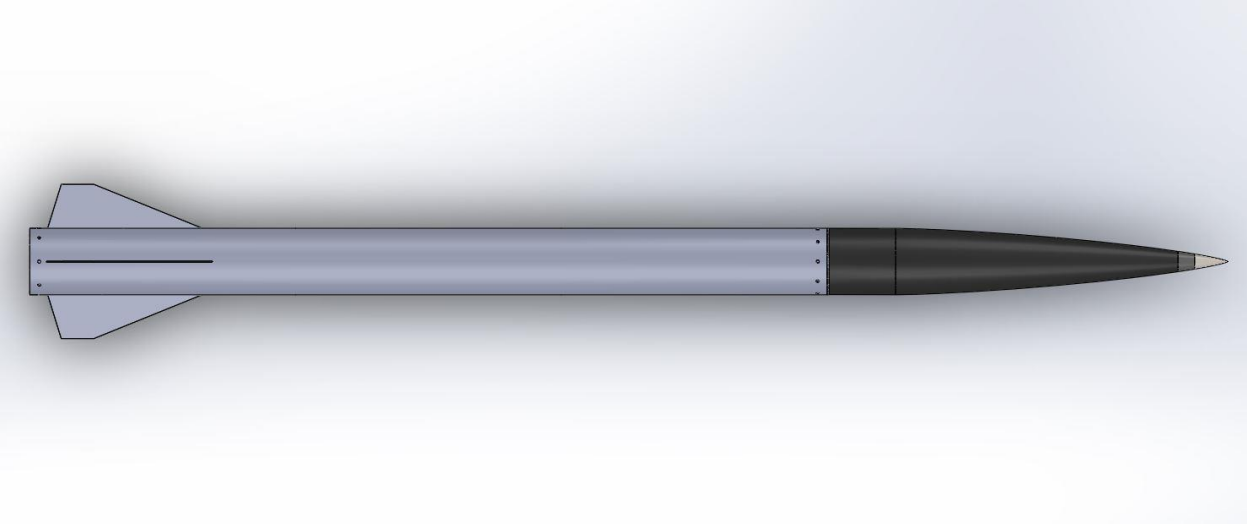

Figure 1: *8-inch diameter final rocket.*

It will be necessary to test at least two motors on our way to building the big motor for the final rocket. The tip of the nose cone we plan on building out of titanium and stainless steel since the tip will experience the most heat and the fiberglass would be at a high risk of delamination at that point. The nose cone will be filament wound fiberglass using the X winder and will double as our payload section where the parachutes, cameras, and electronics will be housed. The forward closure of the motor will double as the

mounting point for the nose cone/payload and will be heavily influenced by the rocket we flew at BALLS 28. The motor casing closures will be secured using grub screws due to their low profile allowing for better aerodynamics. The nozzle will be made from graphite and the carrier will be made from aluminum. They will be secured using the same grub screws as used to secure the forward closure. The fins will be made of aluminum and we will affix them directly to the motor casing in a way that will not affect the temper of the aluminum.

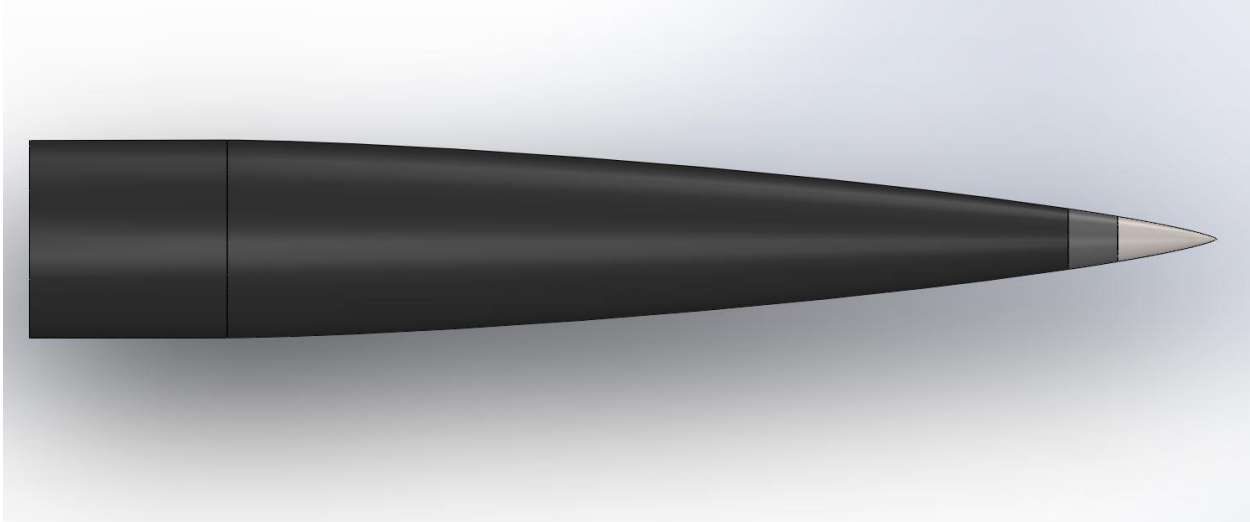

Figure 2: *5:1 Von Karman 8-inch nose cone for final rocket.*

Motor Hardware

Designing two casings that are incremental steps towards what we want to do will be necessary. We will use these motors to test the pressures and temperatures that we can expect to see in the final motor. For everything up to this point we have been using standard snap ring casings and casting tubes/liners so building these cases will be very a new challenge and will prepare us for the final case we need to build. We will also be using a new technique with these larger motors called case bonding. This technique adheres the propellant to the inside of the case with some kind of protective layer in between the

propellant and the case so the case does not burn through. Both the screw in closures and case bonding are expandable to a motor of whatever size we want to build and are in fact very similar to how NASA builds the solid boosters.

From the aft end forward, the grub screws are holding in the nozzle carrier, there are three fins affixed to the motor casing, the forward closure is being held in by grub screws as well, and the nose cone has the stepped metal tip.

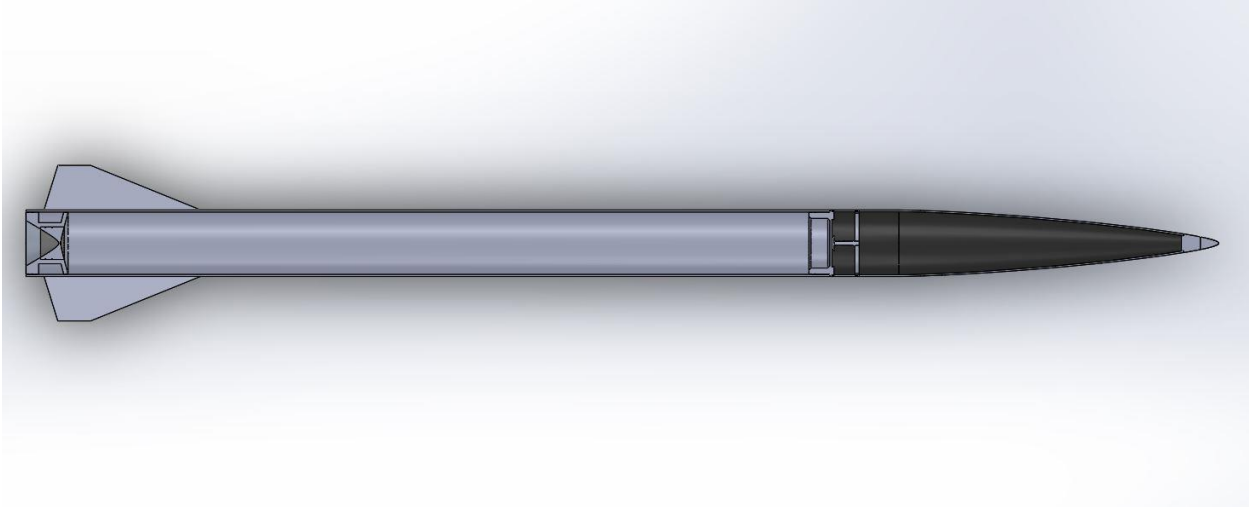

Figure 3: *Cross sectional view of the final rocket.*

Motor Casing

The motor casing is the largest component of both the airframe and motor. This cylinder must withstand the internal pressure of the motor and the longitudinal forces exerted as the rocket travels into large Mach numbers. Fortunately, the internal pressure of the motor and the pressure on the front end of the motor casing will be opposite each other and the aluminum casing will be more than strong enough for the compressive forces. The internal pressure is going to be the main force that we are concerned about. This pressure, in combination with the temperature rise, due to the motor burning inside, will be a large

issue that we must face. For the time being, we will use FEA in SolidWorks for simulating the pressure. Figure (4) is a standard length of tubing that has a standard wall thickness, and it is showing more than strong enough for this flight.

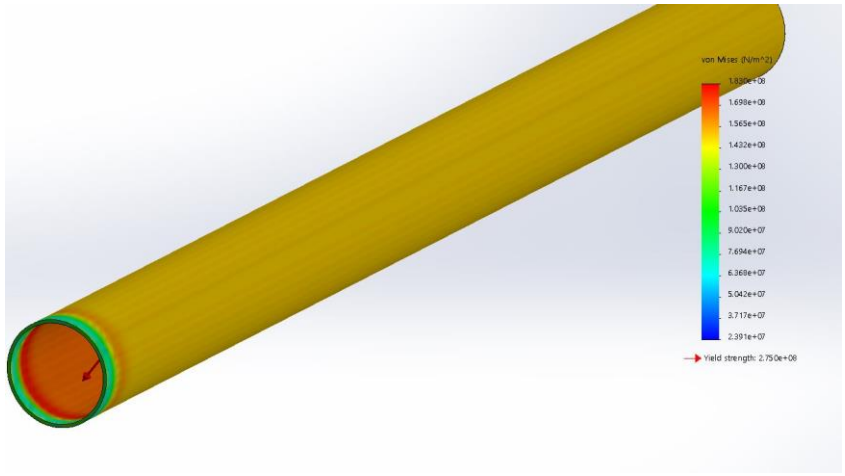

Figure 4: *This model was run at 150% the expected maximum pressure and has a safety factor of 2. Analysis of the closures and attachment of the closures will still need to be done in the future.*

This will also be done to find the strength of the closures. The closures will be made from aluminum and will have strength comparable to the rupture strength of the cylinder. In this case we will design the "weakest" point to be the nozzle end, so we may control the potential failure mode. The thinking behind this is that if the motor over-pressurizes then the nozzle will shoot out and the rocket will be mostly undamaged. This will allow recovery to still work and data from the flight computer to still be collected.

Original Fins

The design for the fins will continue to change as the rocket comes together, but the principles that we use to design them will remain constant. For these very large velocities

many things must be considered. If the fins are tall, extending far from the motor casing, then they could begin to vibrate until they fail and come off the rocket. Extra area also increases drag, so making the fins as small as possible will be very important. The current thinking is that by taking the fin design that we have been using and moving the fin tip aft this will allow for the center of pressure of the fin to also move back and maximize the fin's effect on the center of pressure of the rocket. This has the added benefit of allowing us to make the fins have a smaller surface area and be shorter, solving all the issues we are faced with. The fin designs will be designed in Open Rocket and then put into a fin simulation software to find the maximum speed that we can fly with the proposed design. This software is commercial and finds the velocity that the fin will begin to vibrate at. In Figure (5) we can see that the effect of pulling the area as far back as possible can have similar results to the stability with a smaller area.

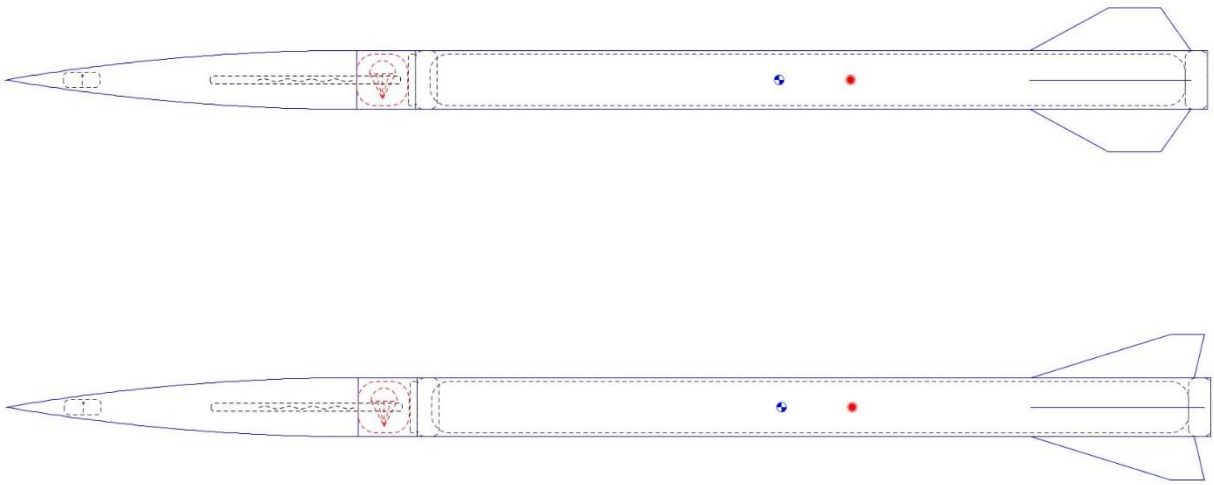

Figure 5: *The two rockets simulated in Open Rocket have a stability that is very close to the same, but the second rocket has a 10% reduction in surface area resulting in lower drag.*

Modified Fins

When it comes to fins, the design must account for the high temperature, high windspeed, and high frequency vibration. They will have the largest area towards the back to maximize effect of shifting CP. They will be made of aluminum that is affixed to the motor casing. Aluminum will be the best choice for fin material due to its high melting point and relatively low weight. Further analysis will determine theoretical maximum temperatures we can expect on the leading edge of the fins. Aluminum will be able to withstand the temperature better than the composite alternative. Also, the high velocities that we are aiming for will cause some issues including vibration in the fins that could cause the fins to fail. Making the fins shorter and closer to the body of the rocket will increase the resonance frequency and increase the velocity that this velocity would occur at. We will also need to find the theoretical best shape for the fins using subsonic testing in the wind tunnel. These shapes that we test will also be tested in commercial fin flutter software at our target velocity. From these tests we will find the fin shape that gives the best efficiency with the lowest chance of flutter. Also, designing the fins to have the largest effect on CP per unit surface area will help determine the fin sizing. This will be the largest factor in designing the rocket and will account for the loss of propellent throughout the burn. Aiming for an initial stability of between 1.2 to 1.8 calibers (rocket diameters) we will be able to size the fins to get the exact stability that we want during the powered portion of the flight.

The fins have been complicated to analyze because of complexities in the harmonics of the fins and how they resonate with velocity. Depending on the fin geometry, attachment method to the rocket, and the material, the flutter velocity will change. The flutter velocity is the resonance frequency of the fins, and how the fins interact with the air as they pass through the fluid. As the Mach number rises, the air behaves more and more as a viscous fluid. This interaction becomes important for our fin design when the Mach number reaches greater than 2. This rocket will go faster than Mach 3 so this will be analyzed with the available tools. We will primarily be using the FinSim software to do this analysis. The reason for this software is that the interactions between the velocity and the resonance frequency is beyond the scope of our undergrad degree. Having said this, the fins that we used for the BALLS rocket this last year were a very robust design for the vibration, but the fin design is not very efficient. A different fin design will be necessary for a faster and more efficient rocket. To make an efficient fin the center of pressure must be as far back on the fin as possible, because the center of pressure of the entire rocket is so heavily dependent on the fins. This means that similar to affecting the center of gravity of a system of masses on a bar by moving a mass further away and therefore increasing the lever arm for that mass and increasing its impact on the whole system. The center of pressure can be seen in the same way, as a series of center of pressures, all with some lever arm from the total center of pressure. This means that by moving the fins backwards that they will have a greater impact on the CP per unit area. That being said, we are looking for a shape that has the smallest area but the largest impact on the center of pressure. The design that we have settled for is a convenient shape that we can take from the existing fin can, that we know is easily capable of withstanding high velocity. We will modify the fins to get this shape.

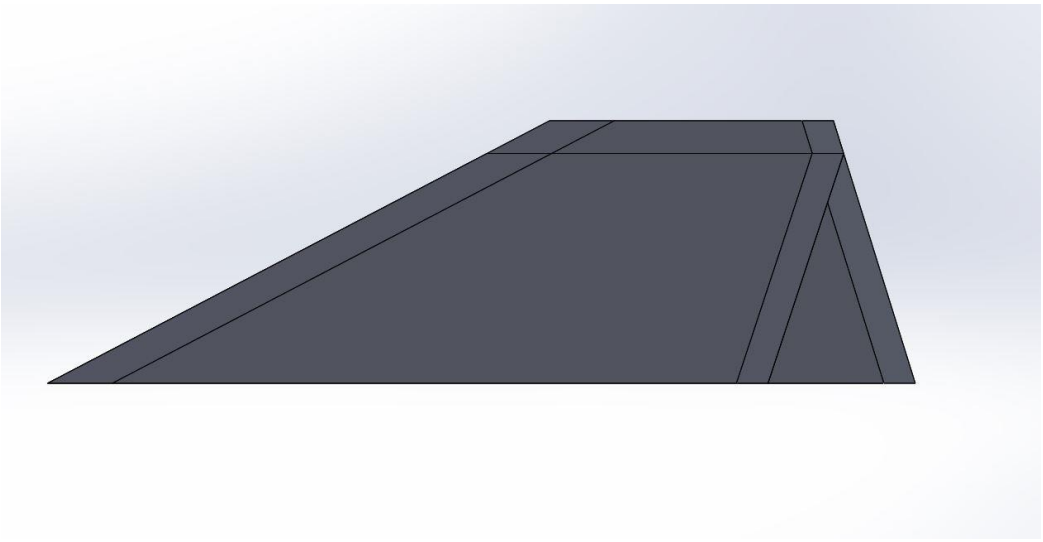

Figure 6: *Old fin with new fin cut away.*

This new fin will reduce the surface area by 11% and has a more efficient design for the actual shape. Also, it will lighten the rocket by reducing the size of the fin and reducing the length of the fin can.

Fin simulation software shows that with the new fin design that the fins will flutter at a Mach number of 4.74 and the ultimate failure velocity will be 6.45. These numbers are not 100% accurate, but they do give an estimate and a confidence. They show that the fins should be fine at a much higher Mach number than we will function at. These numbers will also be in an idealized situation and any perturbance will cause a greater deformation in the fins. Also, the rocket will encounter some angle of attack and the force on the fins will be larger than predicted by the software. This will be compensated for by having a substantial safety factor in terms of velocity.

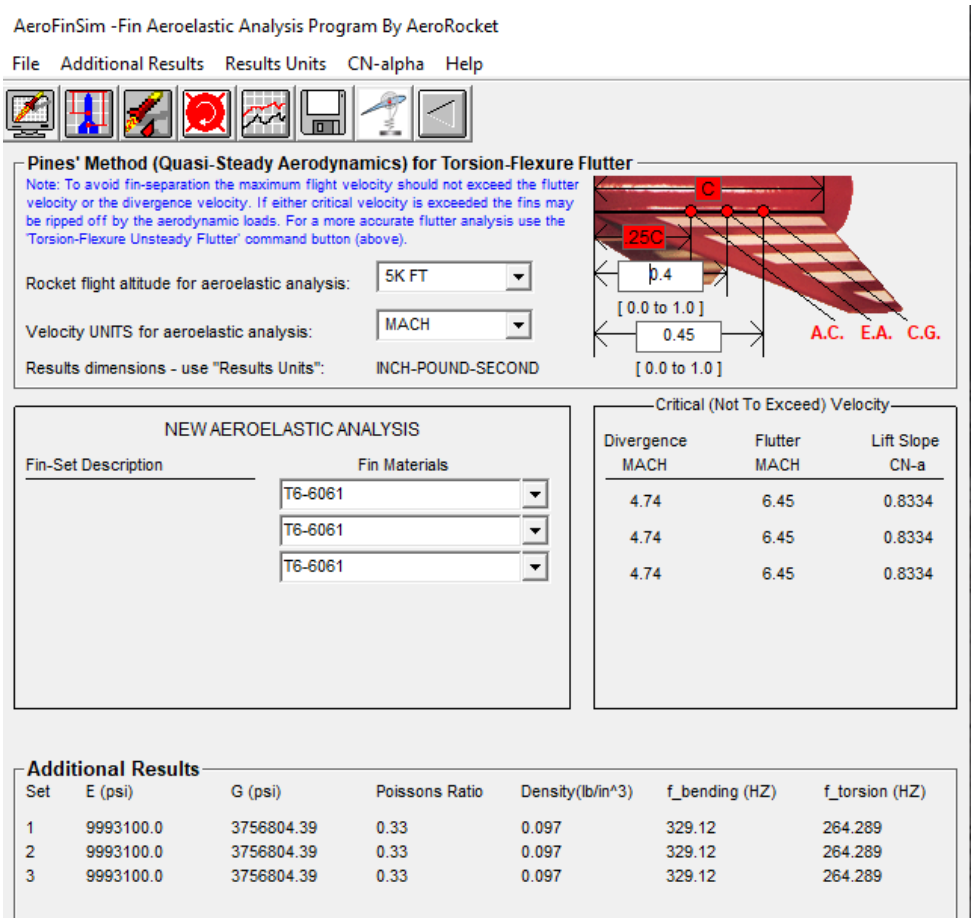

Figure 7: *Fin analysis and divergent Mach number.*

Ejection Charges

These charges will be what actually separates the rocket at apogee, and this alone will require many hours of testing. The rapid creation of gas is the goal of the charges, but many things will affect our gas production rate and efficiency. The altitude will be the largest hurdle to overcome and this is why we plan on building a vacuum chamber to simulate the high atmosphere. This will allow us to make and test as many charges and types of gas generation that we want to. From what we have researched, tested, and flown, black powder will be our most likely candidate. These Black Powder charges will be housed in machined “charge wells” that will contain the gasses and burning powder for long

enough for a full combustion of powder to take place. We will test various shapes to find the smallest size that is able to achieve full combustion.

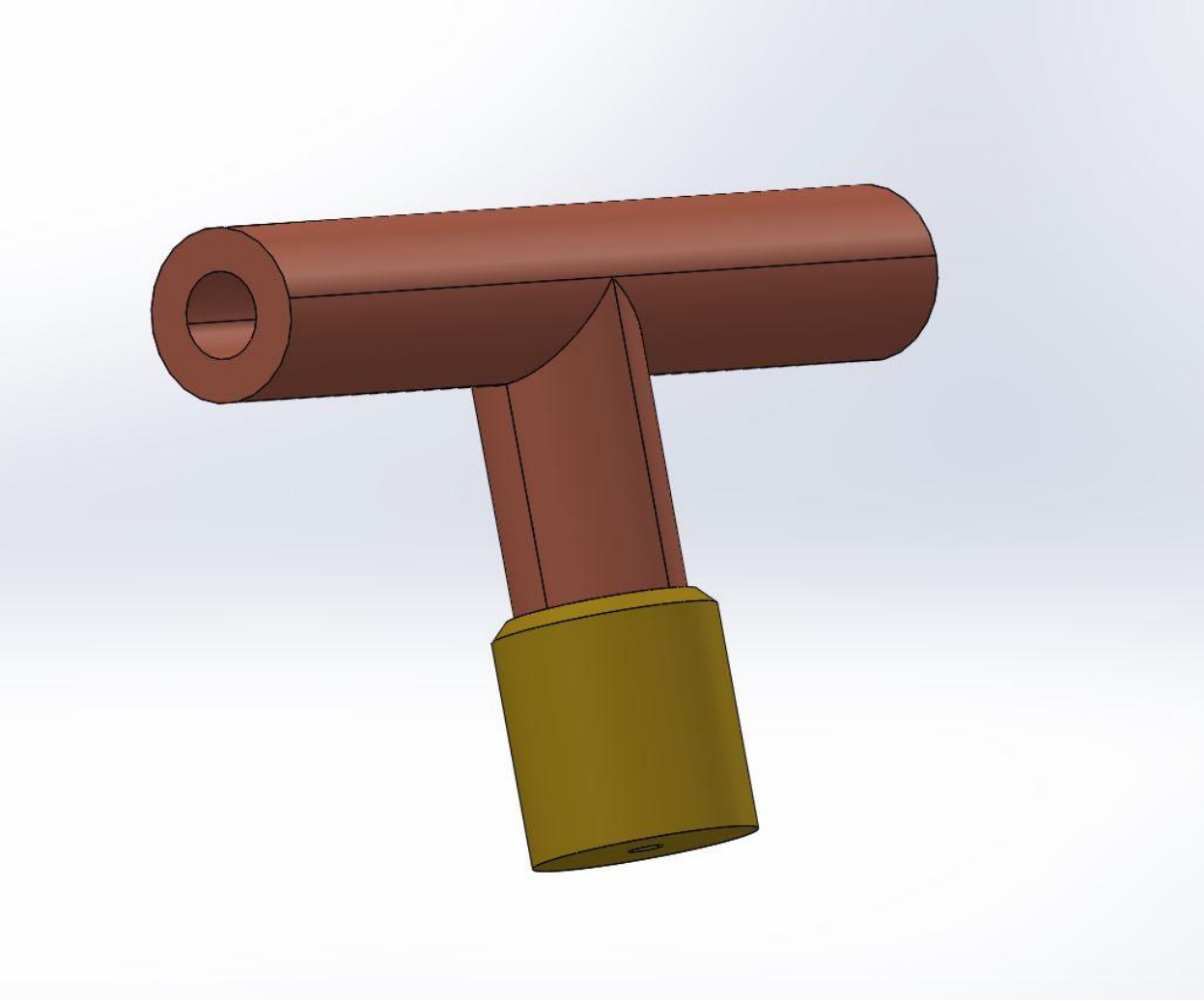

Figure 8: *Brass tee charge that is used for high altitude ejection charges.*

Original Forward Closure

The forward closure must be simple in design, robust, and light weight. We are looking at making the forward closure and coupler section to the nose cone in one part. This part will need to hold pressure and withstand a substantial heat during the thrust phase, along with being the attachment point for the nose cone/ payload section. This will

be more light weight and allow for a very secure connection between the nose cone and motor. This will also be a bolt on or “Frankenstein” attachment style and will have a forward ring similar to the rocket launched at BALLS recently. This design did well practically and was easy enough for us to manipulate in the rocket. This shows that a well thought out and thoroughly simulated part will also be successful in a larger rocket.

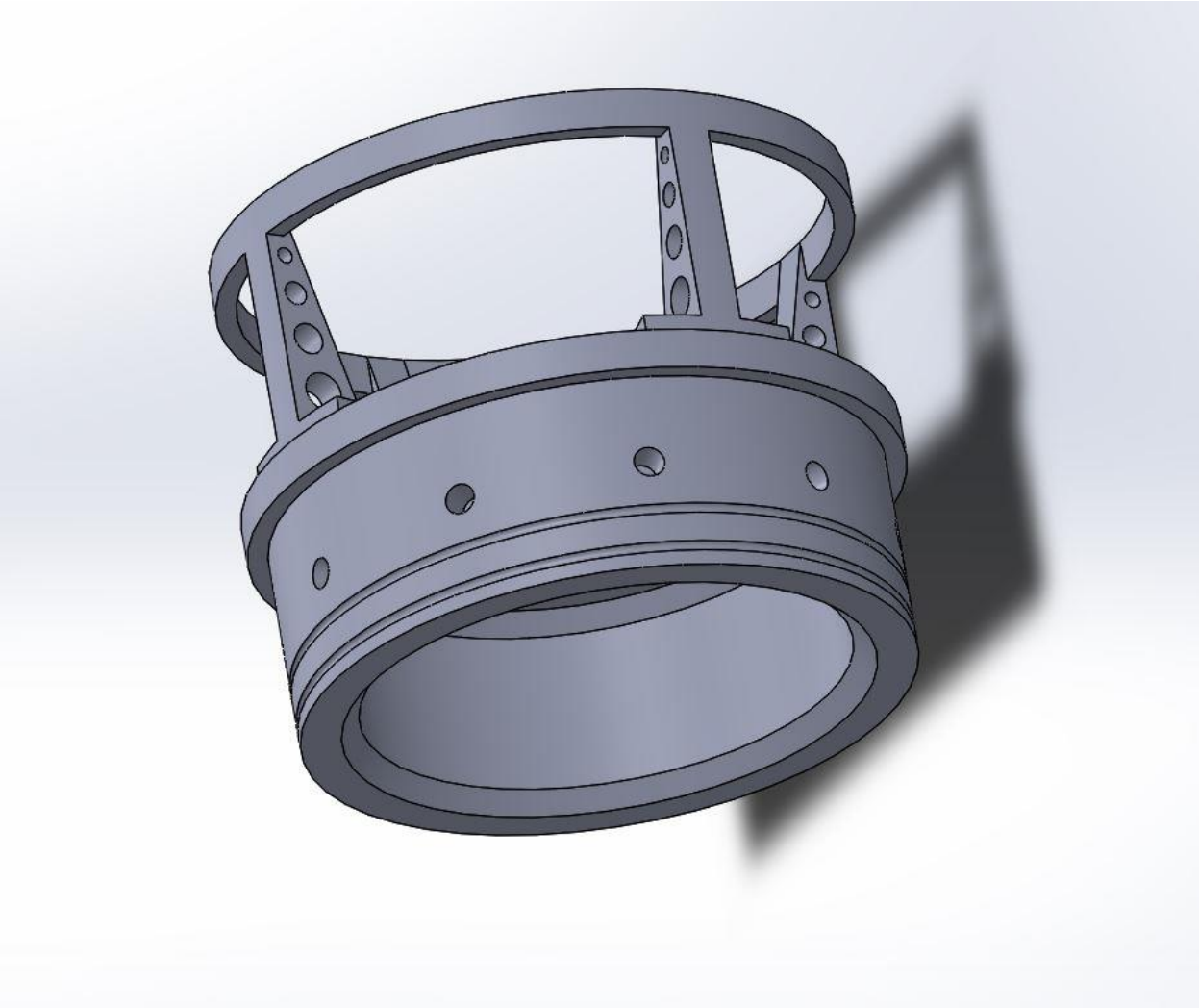

Figure 9: *Forward closure for the final rocket.*

Modified Forward Closure

We also have a new design for the coupling flange that serves to attach the airframe to the motor. The new design is 325 grams lighter than the part used for the BALLS launch and has adequate strength to withstand a 300lbf side load. The fiberglass will be made with a slightly smaller diameter than the BALLS airframe. This is to eliminate the transitional area between the motor tube and the airframe. We have built a mandrel out of MDF in order to make sections of airframe for testing. Our hope is that we will be able to match the strength of factory parts.

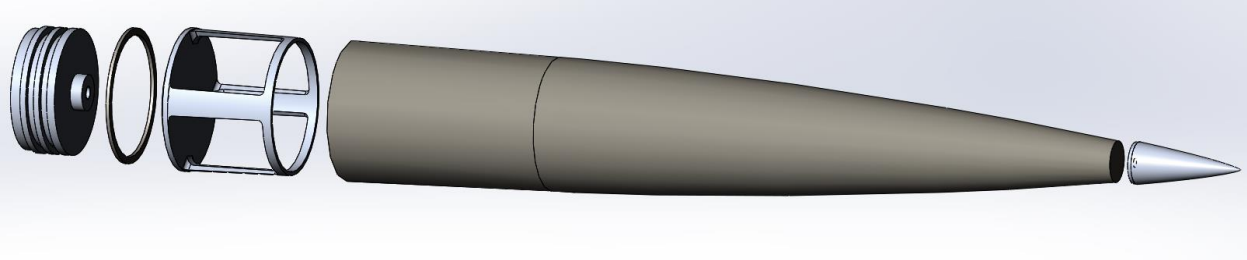

Figure 10: *Exploded view of airframe components.*

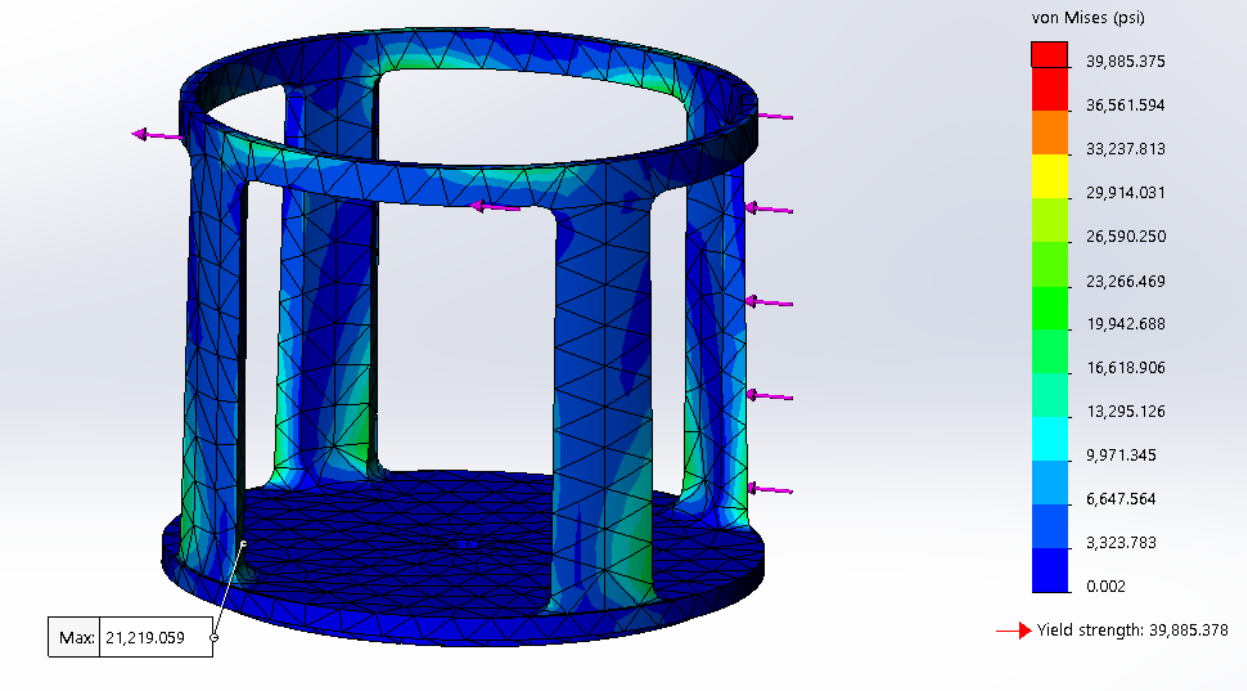

Figure 11: *New Design of Coupling Flange*

The FEA of the coupling flange was done with a 300 lbf transverse load applied. This load was estimated based on the data given by our simulation of the 8-inch motor. This analysis will be updated as soon as we are able to process the data gathered at the most recent motor test.

Launch Tower

We began working on some of the elements of support and logistics that will be necessary for us to launch. We have built a pressure chamber with a pressure transducer which we plan to test ejection charges in. We have also designed a launch tower and have begun the process of applying for a waiver with the FAA and finding a launch location.

The launch tower will guide the rocket in the first moments of the launch until the rocket becomes stable. The design we came up with utilizes off-the-shelf materials for

construction and will be able to adjust for various airframe diameters. The tower will have a fixed external frame that supports adjustable internal rails that will guide the rocket. We will build the frame and rails out of Unistrut and accessory brackets as well as 3/8 all thread. There will be a bottom and a top section of the tower, each 10 feet tall and connected with four-hole brackets. A model of the bottom section is shown in figure (12) with a model of an 8 inch motor tube.

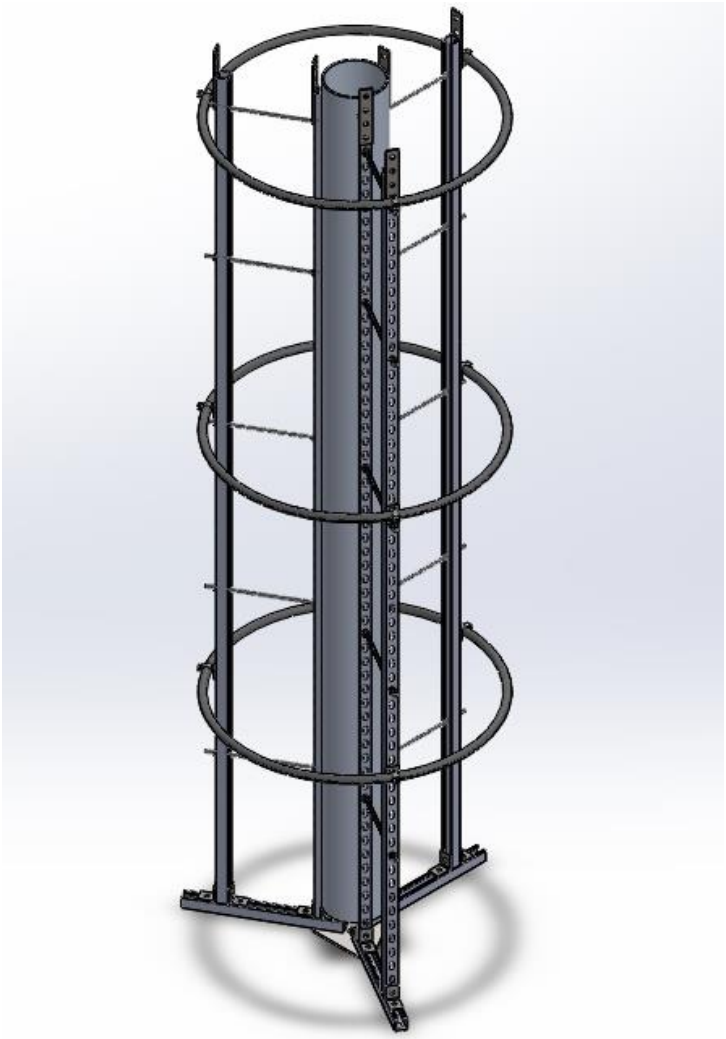

Figure 12: *Model of lower tower section with motor tube.*

Figure (12) is a view of the lower section showing the three rails supporting the motor tube as well as the tubular rings which will give the tower added rigidity.

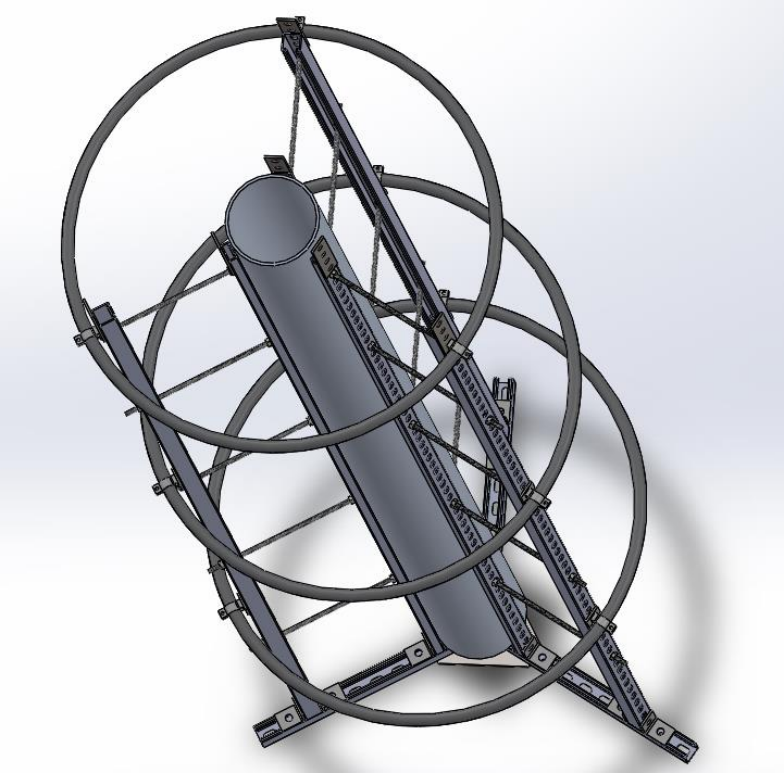

Figure 13: *View of tower rails supporting the motor tube.*

Stakes will be driven through three holes in the base of the tower. For additional support, each frame member will have a 3/16-inch stainless steel cables as guy wires at the midpoint and top of the section. The top section of the tower will have additional guy wires at the midpoint and top. Some changes to the current design may be going from rings to hexagons in order to make manufacturing easier and faster. We also have plans for increasing the stiffness between the outer frame and inner rails using tubing.

Motor Mixing and Testing

Over the course early to mid-2019, we worked on characterizing a propellant. Characterizing a propellant means that you start off with a formula, and you make grains, to then test them in a motor and see what the data looks like. We mixed many batches of a formula we got from Brad McGarvey called Purple Pig. The first few batches were all 54 mm grains that we used in 2, 3, and 4 grain motors. All were successful burns, but the chamber pressure was lower than we wanted it to be. We were running a pressure of about 150 – 250 psi where most propellants run closer to 1000 psi. The next grains we mixed were for another 54 mm, a 75 mm, and a 98 mm. The 54 mm was a 2 grain with a different sized nozzle to allow us to obtain a higher chamber pressure. The 75 mm was a 3 grain and the 98 mm was a 2 grain. After those tests, we were able to characterize the propellant because we had enough data. The first program that was used was ProPep 3 which is a program where you input the formula and then all the information about the grains, and it calculates a burn rate coefficient and a burn rate exponent. Those numbers are needed for the next program that is used which is called BurnSim. In BurnSim, your propellant gets entered and you can enter the grains and the nozzle dimensions so you can test the propellant. BurnSim outputs a thrust curve, the ISP, the impulse, mass flow, and burn time. BurnSim can be used to verify the data from your test burns and it can also be used to make larger motors and see what their burn will look like. From the test burn data, we learned that the propellant was not as energetic as we would have liked it to be, so we plan on modifying the propellant over the next few months. The process of characterizing a propellant was invaluable and it will allow us to characterize a new one much more efficiently.

Formula X Characterization

After BALLS 28, we decided we needed a more energetic propellant to be able to achieve our goals. We started working on new formulas and talking with experienced people in rocketry and developed a formula that we think is the best for our situation. We spent a week mixing small batches to try to figure out the ratio of liquids to the curative so we would have complete cure. Then we made five pucks with a propellant diameter of 2.88 inch and a length of 1.00 inch. We were lent a ballistic evaluation motor which was a thick-walled cylinder with closures and a spot for interchangeable nozzles. We machined nozzles with different core diameters and no divergent or convergent cones. We wanted to have five different nozzles so we could have five different Kn values.

$$K_n = \frac{area\ of\ burning\ propellant\ surface}{area\ of\ nozzle\ throat} \quad (1)$$

Table (1) shows what the values of Kn are based on the nozzle throat.

Table 1: *Calculations of Kn for ballistic motor.*

Propellant Diameter [in]	Nozzle Throat [in]	Area Propellant [in^2]	Area Nozzle [in^2]	Kn
2.88	0.1875	6.514	0.0276	235.9296
2.88	0.1719	6.514	0.0232	280.7757
2.88	0.1563	6.514	0.0192	339.7386
2.88	0.1406	6.514	0.0155	419.4304
2.88	0.1250	6.514	0.0123	530.8416

After running the five test burns in the ballistic motor, we sorted through the data and plotted pressure vs time. One of the burn graphs is shown in figure (14).

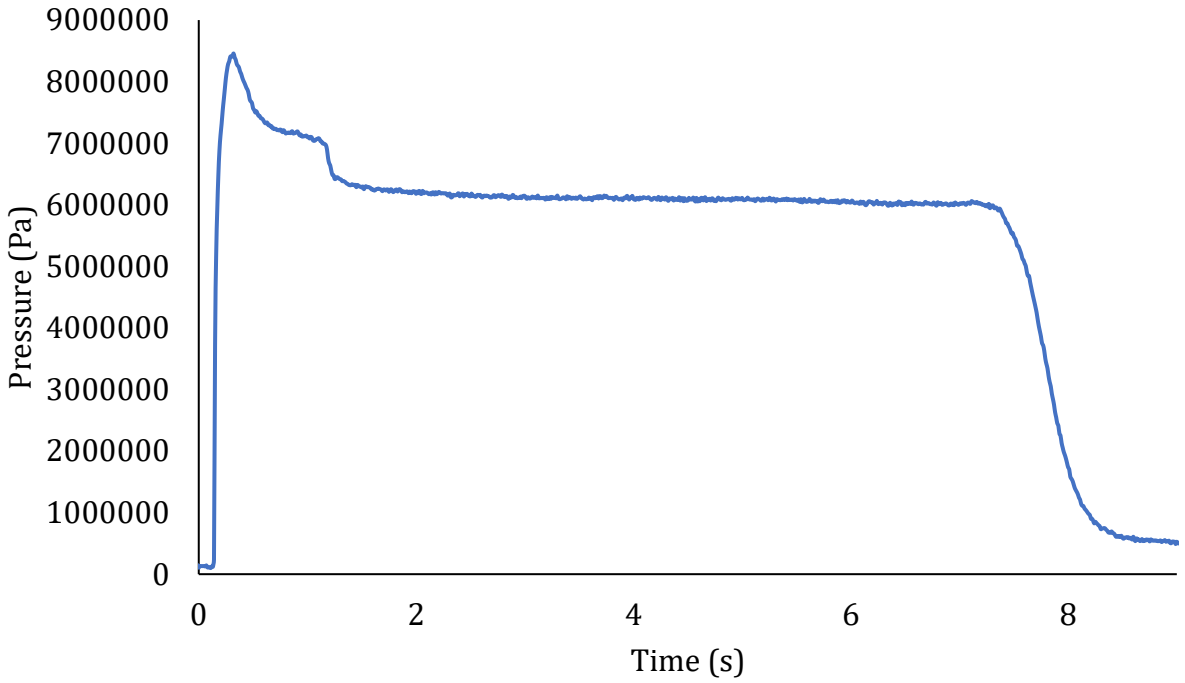

Figure 14: *Pressure vs Time graph for one of the test burns.*

To find the average pressure over the course of the burn the square wave portion is analyzed. To find the burn rate the "turn on" and "turn off" are found and the two times are subtracted, and the length of the grain is divided by the time. Once the burn rate is found, the propellant can be characterized. Table (2) represents the inputs to calculate the isp* and figure (15) represents the output.

Table 2: *The inputs are Kn, pressure, burn rate and isp* is the ouput.*

	Kn	psi	burn rate	isp*
Test 1	235.9296	489.6478	0.1251	255.1356
Test 2	280.7757	495.1629	0.1419	191.1766
Test 3	339.7386	581.1354	0.1515	173.7100
Test 4	419.4304	762.8155	0.1564	178.9174
Test 5	530.8416	889.6208	0.1577	163.5285

Figure (15) is a logarithmic plot to find the burn rate coefficient (a) and the burn rate exponent (n).

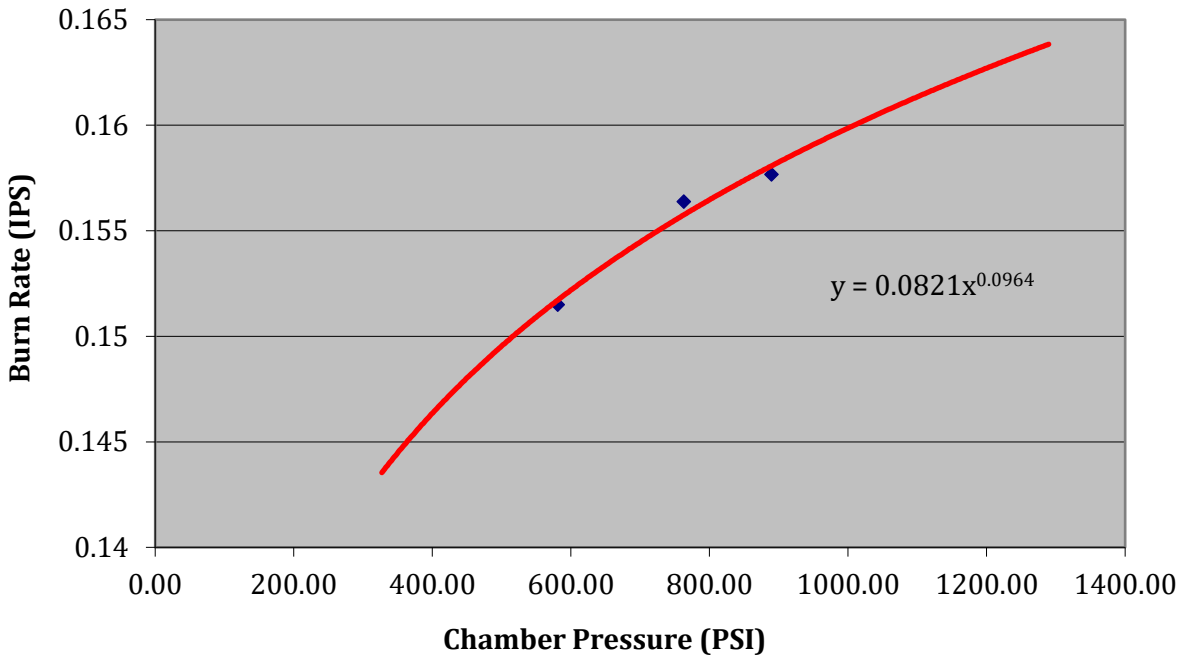

Figure 15: *Burn Rate vs Chamber Pressure graph to calculate a and n.*

Once the *a* and *n* are found they can be put into Burnsim and any motor can now be designed, and the results will be very accurate.

Original Final Motor

The 8 inch motor was designed in Burnsim and we scaled it down for a 4 and 6 in test. Over Fall Break, 60 pounds of propellant was mixed, and casting tube and liner was ordered. We have both the 4 and 6 inch cases and we will be able to pour the grains and test early in the new year. It will be a great test of the new propellant and it will also be good to look at the thrust and pressure data from the tests and compare it to Burnsim and see if anything needs to be tuned to fit how the actual propellant is performing.

Modified Final Motor

After the characterization of Formula X, we realized that this propellant liked high K_n numbers, so we knew we wanted to test the motors at a higher K_n as well. Initially, we were going to test a 4 inch, a 6 inch, and then fly the 8 inch. Due to limitations in our budget, we had to scale back. We decided that we were going to fly the same rocket that we flew at BALLS 28 but with the new, more energetic propellant. We also were going to focus on making the rocket as optimized as possible. After discussing the possibility of different test stand burns we decided we just wanted to test the 4 inch motor which is the same motor that we are going to fly.

The motor was entered into BurnSim and a nozzle throat was chosen based on the pressures. We decided that the profile BurnSim created was what we were looking for and cast the grains based on the dimensions that we had entered into BurnSim. We decided to 3D print casting bases so we could create a dishing on one end of each of the grains to create and standoff so the flame front can get in between each of the grains. This is a traditional Bates grain geometry and usually O-rings are used as a standoff between grains, but we wanted to see if we could create a dishing that would work.

Figure 16: *The 3D printed casting bases.*

Figure 17: *Grains curing.*

After the grains were cast, we weighed and measured all the grains to see how they compared to each other. We also calculated a density of each grain and averaged it to get the overall density of the propellant.

Table 3: *Grain numbers with their lengths, weights, and calculated density.*

grain #	core dia	CT ID	grain L	predicted weight	Recorded weight [g]	Weight in lbs - CT	Calculated density
1	1.25	3.24	4	0.745	0.744	1.5927	0.05674
2	1.25	3.24	4	0.745	0.744	1.5927	0.05674
3	1.25	3.24	4	0.745	0.742	1.5883	0.05658
4	1.25	3.24	4	0.745	0.744	1.5927	0.05674
5	1.315	3.24	7.875	1.439	1.442	3.0854	0.05689
6	1.315	3.24	7.9375	1.450	1.456	3.1155	0.05700
7	1.66	3.24	7.9375	1.280	1.292	2.7539	0.05706
8	1.66	3.24	8	1.291	1.316	2.8061	0.05769

Below are the characteristics of the motor along with the curves and outputs.

#	Length	Diameter	Core	Inhib.	Type	Prop.
1	4	3.239	1.25	0	BATES	Formula X
2	4	3.239	1.25	0	BATES	Formula X
3	4	3.239	1.25	0	BATES	Formula X
4	4	3.239	1.25	0	BATES	Formula X
5	8	3.239	1.315	0	BATES	Formula X
6	8	3.239	1.315	0	BATES	Formula X
7	8	3.239	1.66	0	BATES	Formula X
8	8	3.239	1.66	0	BATES	Formula X

Figure 18: *Grain length, propellant diameter, and core size. Total length of the propellant is 48 inches.*

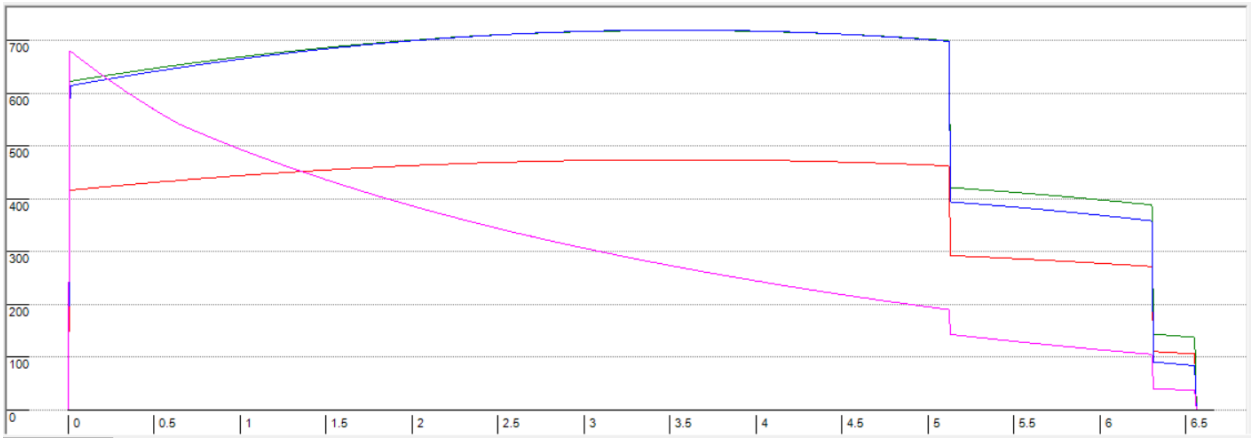

Figure 19: *The blue curve is thrust in pounds, the green curve is pressure in psi, the pink curve is mass flux in lb/s-in², and the red curve is K_n.*

Initial Kn:	416	Burn Time:	6.55 sec.
Max Kn:	474	Propellant Length:	48 in
Max Pc:	718.9 psi	Propellant Mass:	18.19 lbs
Volume Loading:	80.8 %	Total Impulse:	17864 NS
Port / Throat Area:	2.81	Motor Class:	N-2727
Throat / Port Area:	0.356	Delivered ISP:	221 sec.
Core L/D Ratio:	34.1	Peak Mass Flux:	1.36 Grain 6
Web:	0.99 in		

Figure 20: *Outputs from BurnSim.*

Once the data was received from the test, we were able to sort through it. As we have noticed with other motors that we have tested, BurnSim was conservative with the simulation. It is hard to figure out which number is driving why the theoretical does not align with the actual test burn, so the numbers need to be played with until BurnSim aligns better with the actual results. Sometimes, it is not possible to get it to fully resemble the actual motor and that is why testing is necessary to prove how the motor is performing.

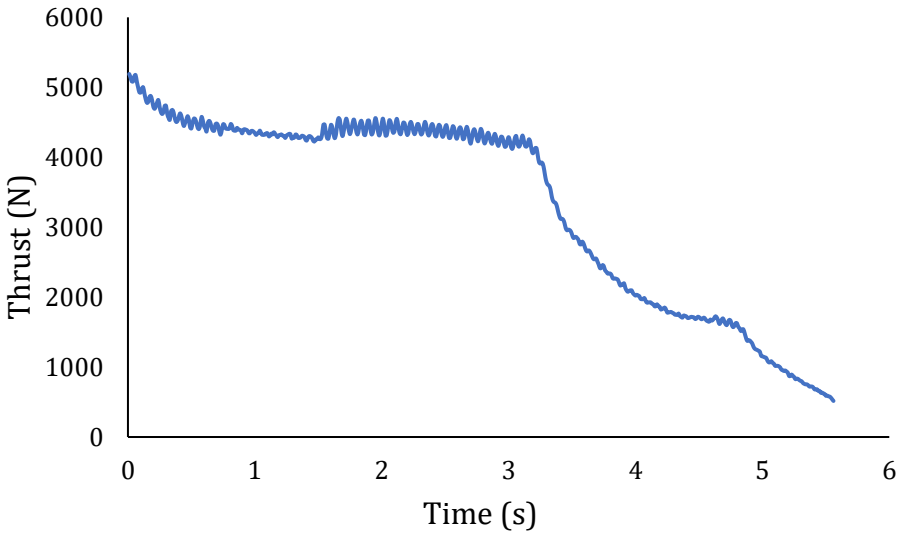

Figure 21: *Thrust vs Time curve from motor test.*

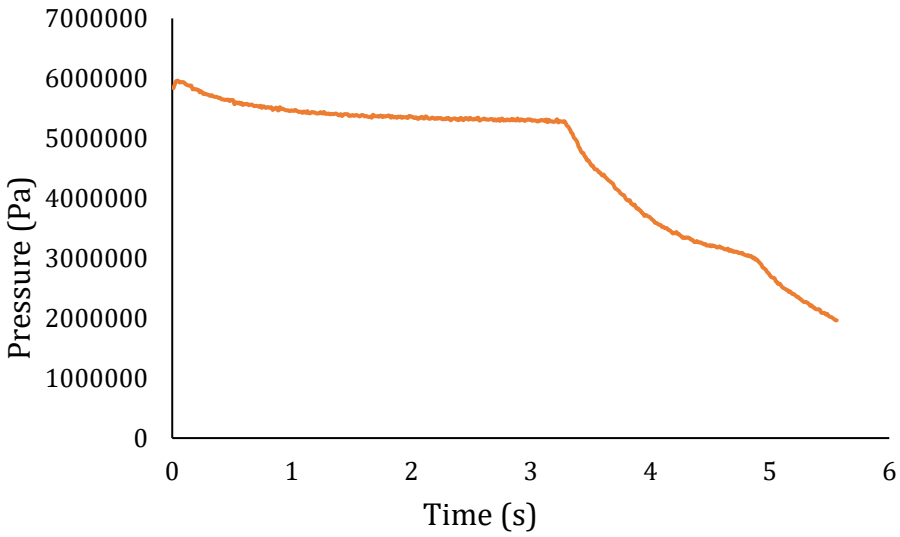

Figure 22: *Pressure vs Time curve from motor test.*

Looking at the difference of the test stand data versus BurnSim it is apparent that the thrust curve is not what BurnSim predicted it would look like. It is similar, and they are both relatively flat burns, but this curve is ever so slightly regressive instead of ever so slightly

progressive. Both curves do produce a good square wave portion and we were very happy with how the motor performed. After going through the data the burn time was 5.56 sec, the average pressure was 664 psi with a peak pressure of 864 psi, the average thrust was 3326 N, and the total impulse was 18,527 Ns. The motor is a 90% N3300.

Figure 23: *Picture of test burn.*

Since this is such a large N, we decided we are going to try for the Tripoli Research Record. The current record is 31,580 feet which we exceeded that altitude already at BALLS 28 with 35,300 feet.

Single Stage N	N-98mm-29in-48in	20480	31,580	5/26/2007	Jim Jarvis,Pat Gordzelik	Electronics:G-Wiz MC, Perfectflite HA-45 *Wayside, Texas* Wayside White Video here: https://www.youtube.com/watch?v=SJEzr4LJyzI

Figure 24: *Current Tripoli N research record.*

Since we did not state we were going for a record then we were not allowed to claim it. According to the simulations, our rocket will exceed 60,000 feet so we had to apply for a unique FAA waiver. We plan on flying out at the Mojave Desert with Friends of Amateur Rocketry from April 25-26, 2020. The process of applying for the waiver was straightforward once we knew for sure that the rocket was considered a Class 2 rocket since the motor is under the P impulse range. The waiver was applied for on February 19, 2020 and we have been in contact with the FAA since then.

Nozzle Analysis and Design

In the early phases of MACH Rocketry, our team has experimented with different nozzle sizes during test burns and other high-power flights. Iterations of tests were completed to ensure that the most efficient nozzle would be used for our final design. This derived from computing chamber pressures generated by the ignition and burning of the propellant and the throat diameter of the nozzle. Our first test burns of the propellant designed and characterized by our team showed a low chamber pressure which resulted in a small amount of thrust. By decreasing the throat diameter of the nozzle, the chamber pressure will increase, creating a more powerful thrust out of the rocket and ultimately propelling it to higher altitudes.

In order to properly design and test rocket nozzles, it is important to understand the theory behind the part. The nozzle is designed to take hot gases and exert them out the opposite direction of desired flight as fast as possible. This forces the rocket to fly directly up at extreme speeds. The solid rocket propellant, sitting stationary in the casing, is ignited and the fuel is burned creating hot gases that need a place to escape. The nozzle is designed to let those gases flow smoothly into the entrance and then through the nozzle throat. The nozzle then diverges into a larger diameter. This geometry allows the hot gases to exert force on the nozzle walls and the mass flow rate to speed up beyond Mach 1.0. The ideal nozzle pressure will equal the atmospheric pressure at the exit of the nozzle cone, creating a rectangle-like shape of mass being exerted out the aft end and forcing the rocket forward at its most efficient rate. The dimensions of the nozzle are crucial to this effect and will be calculated and characterized for our final rocket design.

Our team began by testing rocket motors on a smaller scale in order to ensure the fuel mixture was mixed appropriately and would successfully burn. Once the data from these test burns was gathered and analyzed, the process was repeated on a larger scale. After multiple tests, the fuel was completely characterized, and the rocket motor was ready for flight. The nozzle dimensions were determined following this process given the chamber pressure data. The initial tests of the smaller motors produced low pressures around 200 psi. This needed to increase in order to produce a large amount of thrust. The nozzle throat was then decreased to 1.172 in. to restrict the mass flow rate entering the convergent section of the nozzle and increasing the Mach number in the divergent section. The chamber pressure of the motor for BALLS 28 was about 650 psi according to BurnSim which was suitable for our

launch. The flight was successful, and the motor produced a total impulse of approximately 14,000 N-s, and 742 lbs of average thrust.

The future design of the rocket will be on a much larger scale and therefore will need a significantly larger amount of thrust. The nozzle will be crucial in determining the correct amount of thrust needed. The design of the nozzle will consist of a 6 in cylindrical piece of graphite, which will then be machined, creating the convergent and divergent sections. The nozzle will be held in place by nozzle carrier group. The outside diameter will fit directly into the inside diameter of the rocket motor casing. The nozzle carrier group will be machined out of 6061 T6 Aluminum and will be held in by 6 set screws placed evenly around the cylindrical shape. The nozzle will fit inside the carrier group, ensuring the nozzle will not be forced out of the aft end of the rocket during flight. There are a few considerations when designing the nozzle and nozzle carrier. The main consideration will be the thermal expansion properties of graphite and aluminum. If they expand at different enough rates then the nozzle could become dislodged in the carrier, causing the thrust to be affected. Another consideration for this design is the quality of the graphite. There are many different qualities of graphite that can be purchased from manufactures. These include, very fine, fine, and rough. Each quality has advantages and disadvantages, and these must be considered when designing the nozzle. The rough graphite is the most cost beneficial but the lowest quality. The very fine is the most expensive of all the options but has the finest detail. These design limitations are crucial to the performance of the rocket nozzle and will be considered in the final design.

In order to ensure the best nozzle design for the rocket there will be iterations of testing and machining. Our team will be purchasing a smaller diameter section of graphite to machine and test in a rocket motor. Before the machining process begins, the team will test a 3-D model in SolidWorks using the flow simulation tool. This will give the team valuable data for entrance length, throat diameter, throat length, and exit length. Following computational analysis, the team will machine the nozzle and test the product in a motor burn test. Solidifying the machining process and gathering critical data, our team will be able to move forward with the final nozzle design.

Original Final Nozzle

The nozzle is a critical element to the final performance of the rocket and has been analyzed extensively. The geometry of the nozzle is crucial to its performance and that has been the main design concern. From the propellant testing, certain characteristics have been determined such as Kn values, chamber pressures, burn time and Cp/Cv values. We have created a program to calculate the throat diameter of the nozzle from these values. The rest of the rocket nozzle dimensions can be calculated from knowing the diameter of the throat. This is essential to ensuring maximum performance of the rocket in its final launch. We are going to start manufacturing of the nozzles the week of finals. This will be the first step in the chain to creating the nozzle for the final rocket. The first nozzle will be 4 inches in diameter and will be used in a motor test, the next nozzle will be 6 inches and will be used in a motor test as well, and the final nozzle will be manufactured to be used in the final rocket. The final 8 inch diameter rocket will utilize a nozzle carrier design that will reduce the amount of graphite used and will save money and weight. The nozzle will be bolted into an aluminum hollow carrier to ensure that it stays in the rocket during maximum acceleration.

The nozzle carrier will have a boat tail design incorporated to decrease aerodynamic drag on the rocket.

Modified Final Nozzle

A new nozzle configuration was determined to be essential to the success of the final flight. Multiple iterations of geometries were tested using an online simulator. The theory behind the geometry was established and researched before advancing onto the testing and machining of the part. There were a few concerns with the design of the nozzle geometry including the pressure of the chamber that the nozzle throat creates and the over/under expansion and actual performance and thrust.

The chamber pressure is crucial to the performance of the rocket. This pressure is directly related to the propellant and the nozzle throat dimensions. After running multiple simulations it was determined that the nozzle throat would be 1 inch in diameter. With the new formula for the propellant, this diameter would create a chamber pressure of approximately an average of 700 psi. This is a semi-conservative approach for our rocket. After the most recent motor test the results show a maximum chamber pressure of 864 psi and an average pressure of 664 psi. This is a positive result of the test but can be improved by approximately 100 psi. Simulations were performed in order to determine the new nozzle throat. The new nozzle throat will be more restricting and will have a diameter of 0.97 inches.

Expansion is directly related to the performance of the nozzle and thrust which will ultimately enhance the performance of the rocket. A study of expansion was conducted using the nozzle simulator. This study evaluates the performance of the nozzle using three different geometries. The results are shown below.

Table 4: *1 inch nozzle throat with 15° convergent angle and 15° divergent angle.*

Altitude	Thrust	I_{sp}	State
feet	lbf	sec	
1000	930.01	242.6	UnderExpanded
2000	941.72	243.3	UnderExpanded
3000	953.43	244.0	UnderExpanded
4000	965.13	244.7	UnderExpanded
5000	976.84	245.4	UnderExpanded
6000	988.11	245.9	UnderExpanded
7000	999.82	246.6	UnderExpanded
8000	1011.09	247.1	UnderExpanded
9000	1022.36	247.7	UnderExpanded
10000	1033.63	248.2	UnderExpanded
11000	1045.77	248.9	UnderExpanded
12000	1056.61	249.3	UnderExpanded
13000	1068.10	249.9	UnderExpanded
14000	1079.15	250.3	UnderExpanded
15000	1089.15	250.5	UnderExpanded

MACH # at exit =	2.78	
Avg Thrust =	1010.73	lbf
Avg Isp =	247.0	sec
Max Thrust =	1089.15	lbf
Thrust Coefficient (Cf) =	1.64	(At max thrust)

Table 5: *1 inch throat with 15° convergent angle and 18° divergent angle.*

Altitude	Thrust	I_{sp}	State
feet	lbf	sec	
1000	936.158	244.2	UnderExpanded
2000	948.78	245.1	UnderExpanded
3000	961.411	246.1	UnderExpanded
4000	974.04	247	UnderExpanded
5000	986.66	247.9	UnderExpanded
6000	998.716	248.6	UnderExpanded
7000	1011.342	249.4	UnderExpanded
8000	1023.395	250.2	UnderExpanded
9000	1035.448	250.8	UnderExpanded
10000	1047.5	251.5	UnderExpanded
11000	1060.7	252.5	UnderExpanded

12000	1072.179	253	UnderExpanded
13000	1084.519	253.7	UnderExpanded
14000	1096.285	254.3	UnderExpanded
15000	1106.674	254.5	UnderExpanded

MACH # at exit =	2.96	
Avg Thrust =	1022.92	lbf
Avg Isp =	249.9	sec
Max Thrust =	1106.67	lbf
Thrust Coefficient (Cf) =	1.659	(At max thrust)

Table 6: *1 inch nozzle throat with 15° convergent angle and 23° divergent angle.*

Altitude	Thrust	I_{sp}	State
feet	lbf	sec	
1000	933.389	243.5	**OverExpanded**
2000	947.286	244.7	**OverExpanded**
3000	961.183	246	**OverExpanded**
4000	975.08	247.2	**OverExpanded**
5000	988.977	248.4	**OverExpanded**
6000	1002.096	249.4	**OverExpanded**
7000	1015.993	250.6	**OverExpanded**
8000	1029.113	251.5	UnderExpanded
9000	1042.232	252.5	UnderExpanded
10000	1055.351	253.4	UnderExpanded
11000	1070.026	254.7	UnderExpanded
12000	1082.367	255.4	UnderExpanded
13000	1095.875	256.3	UnderExpanded
14000	1108.606	257.1	UnderExpanded
15000	1119.47	257.4	UnderExpanded

MACH # at exit =	3.16	
Avg Thrust =	1028.47	lbf
Avg Isp =	251.2	sec
Max Thrust =	1119.47	lbf
Thrust Coefficient (Cf) =	1.659	(At max thrust)

The altitude shown in the first column in the three tables is determined from the burn time of the rocket. This is an approximation given that the burn time will be around 5.5 to 6 seconds. It is clear from these results that the largest exit cone angle of 23° has the optimal performance. The thrust is the largest of the three geometries as well as the mach number at the exit of the nozzle. The expansion was also shown for each of the scenarios and it was determined that the data from Table (6) had the best expansion ratios. The optimal performance for any nozzle would have a parallel plume out of the exit of the nozzle giving it a perfectly expanded ratio. In the final geometry of 23° divergent cone angle, the expansion is almost perfectly parallel throughout the majority of the burn. This will produce the highest amount of thrust and will be completely optimized for the final flight.

As discussed earlier, a motor test was conducted to test the new propellant formula as well as the 1 inch nozzle throat with a 15° convergent cone angle and divergent cone angle. The nozzle was machined out of superfine isomolded graphite using the lathe. The cylinder was cut to length and then machined down to the correct outside diameter. The first step to cut the inside geometry was to bore out the nozzle throat diameter all the way through the cylinder of graphite. Once this step was accomplished, the entrance cone was machined. The lathe was set at the appropriate angle and we began cutting in and then reversing the cut outwards. This step was repeated until the exit diameter was the correct dimension. The nozzle was then flipped around and chucked up to begin cutting the entrance cone. This was much longer of a process and took multiple passes. Once the entrance diameter dimension was met, the sanding and polishing process began. We started with 800 grit sandpaper at typical rotating lathe machining speeds and with my finger, carefully pressed the sandpaper onto the inside surface of the graphite nozzle. After multiple passes, we switched to 1000

grit sandpaper, repeating the same steps. The final polish was created using 1500 grit sandpaper and pressing with a great amount of force on the inside surface of the nozzle. This removed any leftover grit on the graphite and created a polished surface finish. This is essential to achieving the optimal performance of the nozzle as well as making post clean up processes easier.

The nozzle performed very well during the motor test. The new nozzle will contain the updated geometry with a 23° divergent cone angle with a 0.97 inch throat diameter. Machining of the new nozzle will begin shortly and will be the final nozzle for the final rocket.

Machining and Analysis

The objective of this project dictates that we minimize the effects of aerodynamic drag on the rocket. We decided to try a sub-minimum diameter design to reduce both the weight and drag caused by a larger diameter airframe. In order to eliminate the lower portion of the rocket which typically incorporates the fins, a motor tube and centering rings, we designed a coupler that makes the connection between the upper airframe and the motor case. We built and launched a rocket as a proof of concept for the design using a 4-inch airframe and motor case. The coupler that we manufactured can be seen in Figure (25).

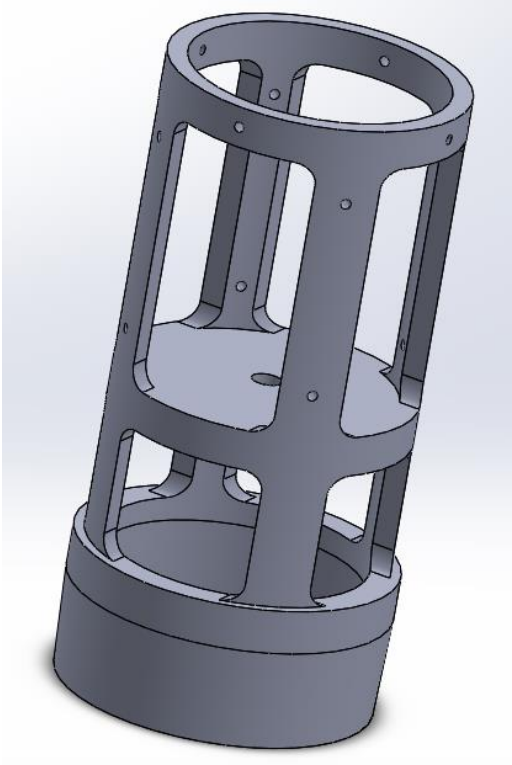

Figure 25: *Coupler used for airframe to motor case connection on a 4-inch rocket.*

This design has a 1.5-inch sleeve which slips down over the top of the motor case. The sleeve caused a step in the outer diameter (OD) of the rocket between the airframe and the motor case. The inner diameter (ID) of this sleeve was machined to match the OD of the motor case with a 0.002-inch clearance. The idea was to minimize the movement between the coupler and the motor to increase the stability of the assembly. The motor case sits flush against a 0.25-inch thick ring that transmits the force of thrust to the rest of the airframe. Analysis of this ring under a 1100 lb. compressive load gave a safety factor (S.F.) of greater than 19. Although a lower S.F. would reduce the weight of the part and increase the altitude of the rocket, strength was our concern for this build. The next iteration will be better optimized to decrease the weight of the part and still maintain a reasonable S.F.

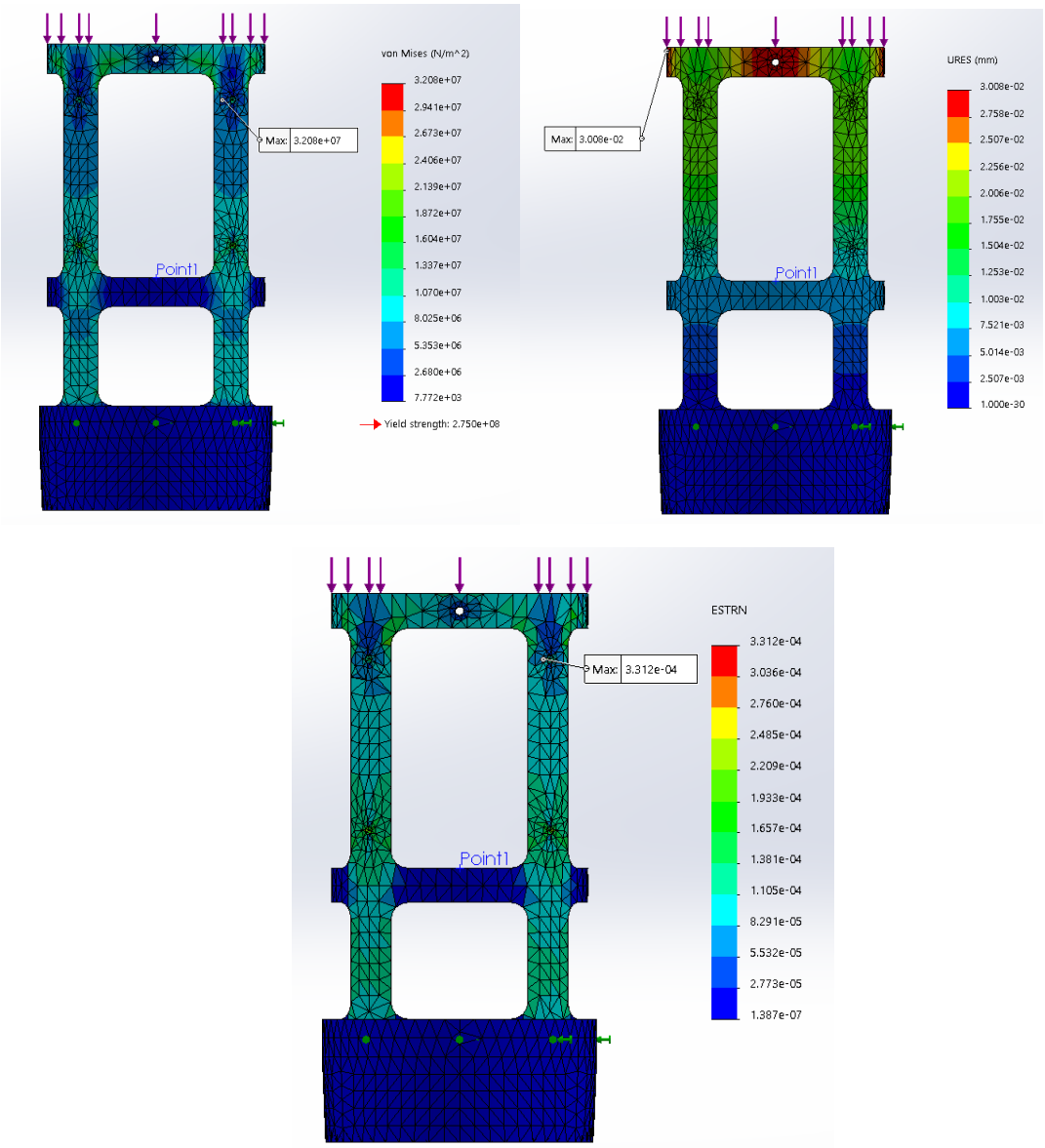

Figure 26: *Analysis done on the coupler that was used for the BALLS 28 rocket.*

A lathe was used to turn the top 6 inches of the coupler down to match the inner diameter of the fiberglass coupler which in turn slid into the fiberglass section of airframe. The inner fiberglass coupler was unnecessary and will likely be revised in the next design evolution to save weight. Both the bottom and top IDs were machined using the same process.

A solid 6061-T6 aluminum cylinder was faced on both ends to ensure a perpendicular surface. The center of the cylinder was then drilled to a 1-inch ID using several drills of increasing diameter. A boring bar was then used to take the ID out to the final desired dimension. Once the inner and outer diameters had been machined our next operation was to drill and tap holes in the upper portion. These holes were tapped with 8-32 threads and were used to attach the fiberglass airframe to the coupler. Windows were machined out of the walls of the coupler using a 0.5-inch end mill to reduce weight.

The design of the final rocket will use a similar method for attaching the airframe to the motor case. The most notable difference with the new design is that the coupler is incorporated into the forward closure of the motor. This is made possible by designing the forward closure with a different method of retention. The previous rocket used a retaining ring in a groove cut into the inside of the motor tube to keep the forward closure in place. The new motor will have a series of set screws threaded into the forward closure, allowing the top of the forward closure to be flush with the top of the motor tube. This feature will allow us to match the OD of the airframe to the OD of the motor case without a stepped or tapered transition. This should aid in reducing the aerodynamic drag and reduce the possibility of bow-shock at the different OD's.

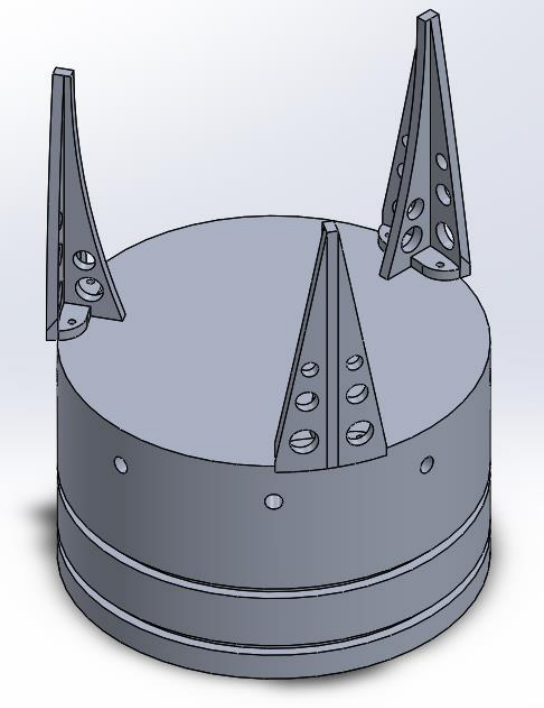

Figure 27: *New concept of coupler designed to match the motor OD to the airframe OD.*

The new design shown in *Figure 19* incorporates rigid fingers which will be bolted to the forward closure. The fingers will be offset from the OD of the forward closure so that the OD of the fiberglass airframe matches the OD of the motor case. Analysis of these fingers under a 1100 lb. compressive load yielded a maximum normal stress of 1626.57 psi and a maximum displacement of 1.7×10^{-5} inches. The forces applied for this analysis were estimated using the thrust applied by the 4-inch rocket. The thrust of the final rocket should be much greater however the load will be distributed to the fiberglass airframe directly with this design. This will allow us to decrease the thickness of the web on the supports. The purpose of the fingers will be to add support in the event of a moment being applied to the airframe. For this reason, it may be necessary to increase the number of supports.

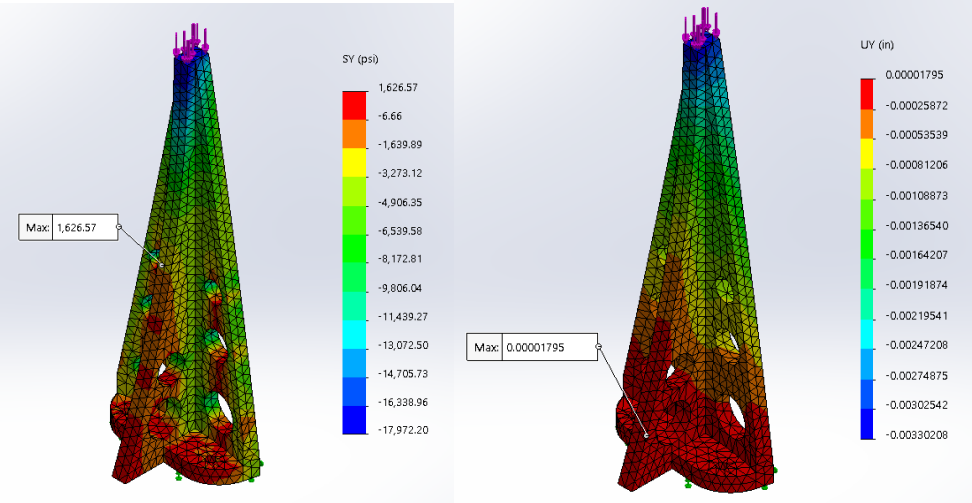

Figure 28: *Analysis of stress and displacement under 1100 lb. compressive load.*

Materials Testing

High power rocketry requires a thorough evaluation of engineering topics including aerodynamics, propellant characterization, nozzle design, electronics, and material design. Material testing and evaluation is crucial to ensuring a successful flight under extreme compressive loads. The purpose of this test was to determine the mechanical properties of multiple materials in hollow cylindrical form to augment and enhance the design of the body tube on our rocket. The three materials, standard cardboard, blue phenolic, and fiberglass tubing, were placed under compression until fracture and the mechanical properties were recorded. These properties were analyzed, and important specifications were calculated to determine the optimum body tube material. The compressive strength of fiberglass, 175.14 MPa, outperformed the other materials by an excellent margin. This value was evaluated and determined to withstand an average thrust value of 90018.35 N. It was determined that fiberglass is the best material for high power rocketry and our design.

There are many aspects to building and designing a rocket. To enhance the performance in each of these categories, the designer must consider the materials necessary. In this portion, material design and testing will be evaluated and discussed. Our team, MACH Rocketry, conducted compression tests on multiple materials to determine the best possible material for our body tube. This can improve strength, aerodynamics and save weight, ultimately achieving a greater altitude. The purpose of this test was to determine the mechanical properties of multiple materials in hollow cylindrical form to augment and enhance the design of the body tube on our rocket.

This test consisted of three separate materials to be evaluated under compression. The materials will be standard cardboard tubing, phenolic tubing commonly referred to as blue tube, and filament wound fiberglass.

The compression tests were conducted using the Instron Machine as well as the certified MTP concrete compression tester. The pre-processing of the materials included cutting down an original 4 feet length tube of each of the materials into smaller sample sizes. The tubes were cut down into 6 in lengths with each material consisting of 4 in diameter sections. The ends of the cylinders were sanded down to ensure a flat contact surface for the testing devices. The exact lengths, inside diameter, and outside diameters were measured before conducting the compression test. The cross-sectional area was then calculated using equation (2) to record and calculate the stress later on.

$$A_c = \pi * \left(\frac{OD^2 - ID^2}{4}\right) \quad (2)$$

Where OD is the outside diameter of the tubing and ID is the inside diameter of the tubing. Once these values were calculated and recorded, the samples were ready to test. The Instron

was used for the first two samples, the standard cardboard tube and the blue phenolic tubing. The Instron was calibrated and the sample was placed into the machine. The software was set to record the extension in millimeters and load in Newtons. The extension rate on the machine was set to 2 mm/min which was later determined too slow and was increased to 10 mm/min. The safety stop on the Instron was set to 25 kN to ensure that if the sample exceeded the limits of the machine, the load cell would not malfunction and break. The heads of the Instron were lowered to right above the sample and then using the small increment adjustment, brought down flush with the top of the sample. The loads were then balanced on the software and the protective door was closed. The compression test was then conducted until the sample failed and the data was recorded. This process was repeated multiple times for a total of 6 samples, three for each material. The fiberglass was then placed into the Instron and tested in compression. The material was too strong for the machine, exceeding the 25 kN load cell, and was determined that it must be tested in a larger, more powerful machine. Our team decided to use the MTP concrete compression testing machine. The samples of fiberglass were placed in the machine and the steel heads were placed on the top and bottom of the sample. The machine was calibrated and began compressing the material. Once the material had failed, the samples were removed carefully, being aware of any fiberglass splinters, and evaluated further.

Materials Selection

Following the testing of the materials under compression, the data was analyzed, and the mechanical properties were calculated. The results from the compression test of standard 4-inch diameter ($D = 101.6\,mm$) cardboard, blue phenolic, and fiberglass tubing are shown below in Tables 1, 2, and 3 respectively.

Table 7: *Comparison of mechanical properties for standard cardboard tubing with D = 101.6 mm.*

Sample	Length [mm]	Thickness [mm]	Area [mm²]	Compressive Strength [MPa]	Elastic Modulus [MPa]
1	151.84	2.06	323.38	10.54	1540.51
2	151.12	1.91	300.26	10.64	1683.60
3	152.76	2.06	323.05	11.05	1354.45
Mean	151.91	2.01	315.56	10.74	1526.20
Std. Dev	0.82	0.09	13.25	0.27	165.02

Table 8: *Comparison of mechanical properties for blue phenolic tubing with D = 101.6 mm.*

Sample	Length [mm]	Thickness [mm]	Area [mm²]	Compressive Strength [MPa]	Elastic Modulus [MPa]
1	152.40	4.57	715.98	24.78	2460.91
2	151.23	3.25	516.66	29.54	2327.43
3	150.93	3.71	577.63	25.92	2505.15
Mean	151.52	3.84	603.42	26.75	2431.16
Std. Dev	0.78	0.67	102.13	2.49	92.52

Table 9: *Comparison of mechanical properties for fiberglass tubing with D = 101.6 mm.*

Sample	Length [mm]	Thickness [mm]	Area [mm²]	Compressive Strength [MPa]	Elastic Modulus [MPa]
1	152.88	3.61	568.86	162.57	6480.16
2	152.12	3.25	513.81	175.14	5116.59
3	152.70	3.40	537.62	157.20	2454.83
Mean	152.57	3.42	540.10	164.97	4683.86
Std. Dev	0.40	0.18	27.61	9.21	2047.26

Given these results and from the calculations of stress and strain from the compression tests of each material, plots were created to show the relationship between stress and strain for the given materials. These plots are shown below for the cardboard and blue phenolic tubing.

The fiberglass was tested in the Instron initially but unfortunately, maxed out the 25 kN load cell's capabilities. Due to this, our team tested the fiberglass samples in the concrete compression machine which only produced a total load applied value. A plot for the fiberglass samples is not available, at this time. Future samples will be wound on the filament winder and tested appropriately, and plots will be created for these results. The compression tests produced the load in Newtons and the deformation in millimeters and from this raw data, the stress and strain can be calculated. The stress is calculated using equation (3).

$$\sigma = \frac{F}{A_c} \tag{3}$$

Where σ is the stress in MPa, F is the load applied to the part in Newtons, and A_c is the cross-sectional area of the sample in millimeters. The strain can then be calculated using equation (4) below.

$$\varepsilon = \frac{L - L_0}{L_0} \tag{4}$$

Where ε is the strain in [mm/mm], L is the length of the sample after deformation has occurred in millimeters, and L_0 is the original length of the sample in millimeters. These values were plotted and shown below for the cardboard and blue phenolic tubing in Figures 1 and 2 respectively.

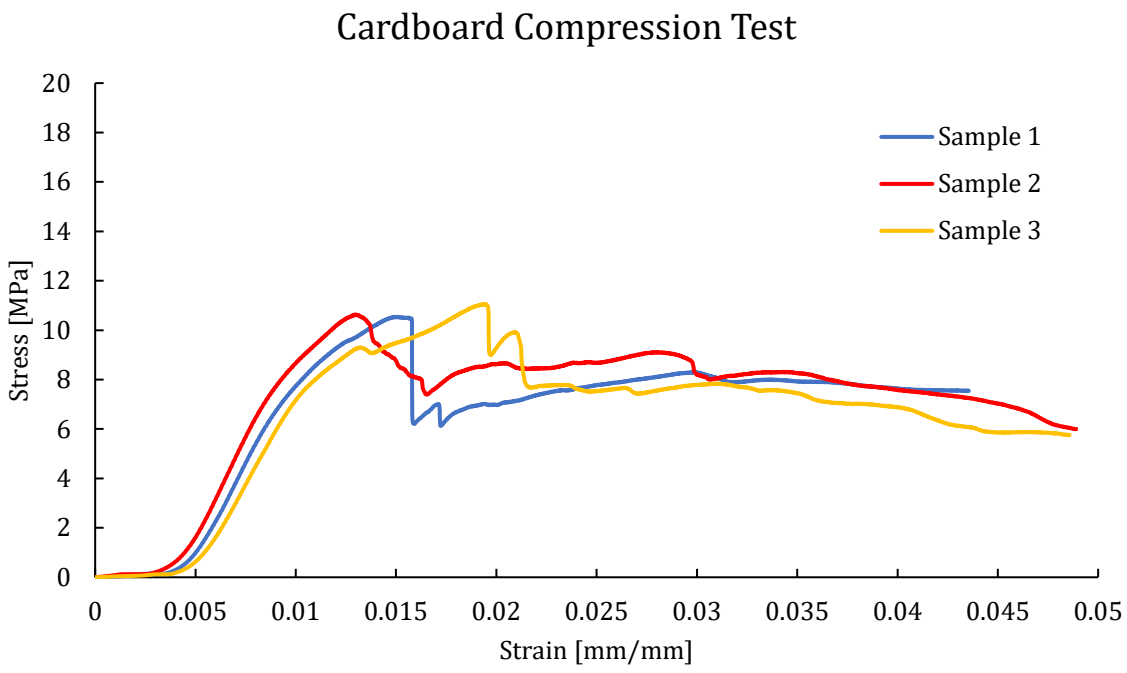

Figure 29: *Stress/Strain curves for three cardboard tubes, D = 101.6 mm, tested in compression.*

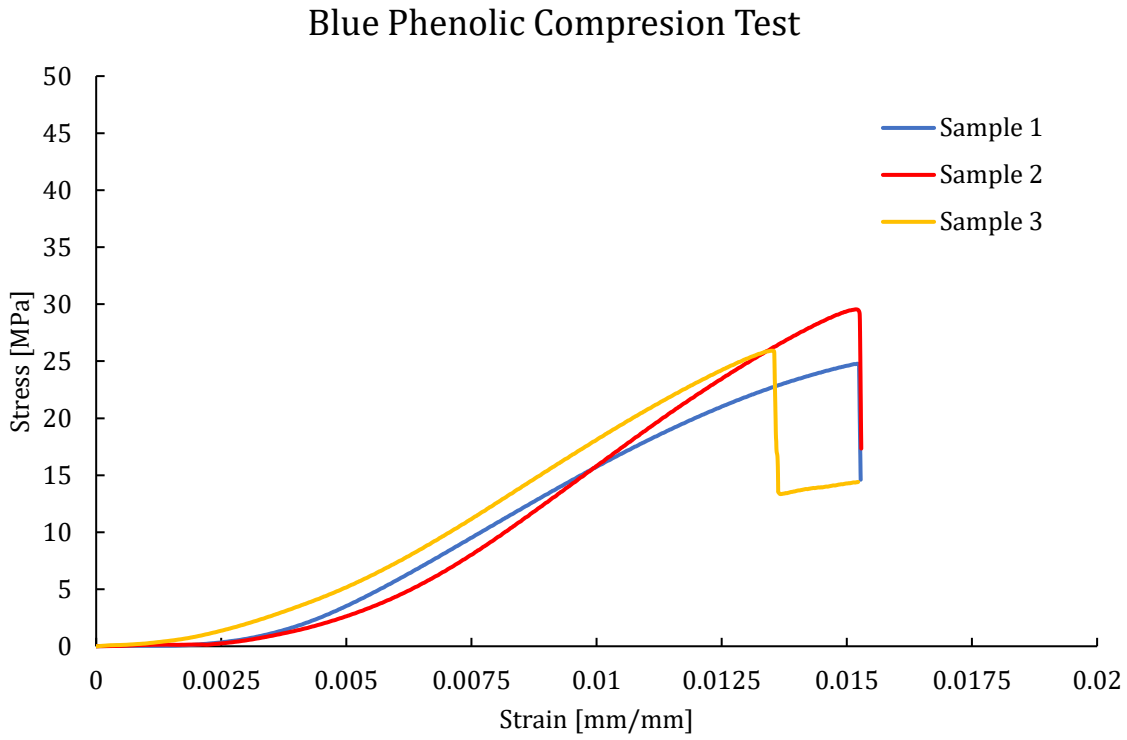

Figure 30: *Stress/Strain curves for three blue phenolic tubes, D = 101.6 mm, tested in compression.*

A comparison of compressive strength and thrust was calculated to show the maximum allowable thrust that each material can withstand. The tabulated results are shown below in Table 10.

Table 10: *Comparison of maximum allowable thrust in Newtons for three different materials.*

Material	σ_{max} **[MPa]**	A_c **[mm²]**	**Max Thrust [N]**
Cardboard	11.0509	300.26	3319.28
Blue Phenolic	29.5440	516.66	15269.43
Fiberglass	175.1379	513.81	90018.35

The purpose of this study was to determine the mechanical properties of multiple materials in hollow cylindrical form to augment and enhance the design of the body tube on our rocket. The strength of these components is critical in knowing how the material will perform under an applied load. The compressive strength is the critical value for a rocket body tube because it is the main force acting on the body during the boost phase. The results from the cardboard tube show a maximum compressive strength value of 11.05 MPa. The results from the blue phenolic tubing produced a maximum compressive strength value of 29.54 MPa. The results from the fiberglass compression test produced a maximum compressive strength value of 175.14 MPa. When comparing these values, the strongest material in compression, is the fiberglass tubing by a large margin. When designing a rocket body, it is extremely important to consider not only the strength, but the weight. The densities of these materials were recorded to be 0.689, 1.75, and 1.45 g/cm^3 for the cardboard, blue phenolic and fiberglass tubes respectively. Cardboard has the lowest density and therefore is extremely light weight, which may be used for low force rocket applications, but when launching high thrust motors, the compressive strength of the material is too weak and can fail during boost phase. Comparing the blue phenolic to the fiberglass is essential, because the densities are similar. The fiberglass tube had a lower density of 1.45 g/cm^3 and a much larger compressive strength value of 175.14 MPa. Compare this to the blue phenolic tubing density of 1.75 g/cm^3 and a compressive strength of 29.54 MPa. The fiberglass is clearly the superior material for large rockets producing extreme amounts of thrust. This initial thrust off the launch rail produces a very large compressive force and the fiberglass is proven to take the force without failure. The fiberglass is also lighter, which is a great advantage for the designing and building of rockets. With less weight, the rocket can travel

to a higher altitude given the same amount of thrust. The maximum allowable thrust for a given material was shown in Table 4 and the results show that the fiberglass is the strongest material for large thrust motors. The maximum allowable thrust value for fiberglass was 90018.35 N. The cardboard and blue phenolic tubing produced maximum allowable thrusts of 3319.28 and 15269.43 N. The cardboard tube works great with small scale motors, typically Level 1 flights with an impulse range of 160.01-640 N-s. The blue tube would be recommended for Level 2 flights or for structural components like couplers or electronics bay tubing. The fiberglass is the strongest material and is recommended for impulse ranges of 2560.01 N-s and above. This is the optimum material for the rocket that our team is designing.

Analysis

A rocket simulation program, Basic_Rocket_Sim.m, was written for the purpose of evaluating the flight dynamics of a mass through its ascent to apogee. The simulation's main focus is to determine the maximum acceleration, height, and speed of a mass with a given motor profile. From this data, forces and then stresses can be calculated on the airframe. The simulation used in conjunction with a mass property program allows an iterative approach for establishing the properties of a rocket that reaches the desired Mach number at a given height. Results from the simulation are also used to forensically analyze data from actual rocket launches and predict the behavior of subsequent rockets going forward. The Dark Star rocket flight data and its known characteristics were used in the first analysis.

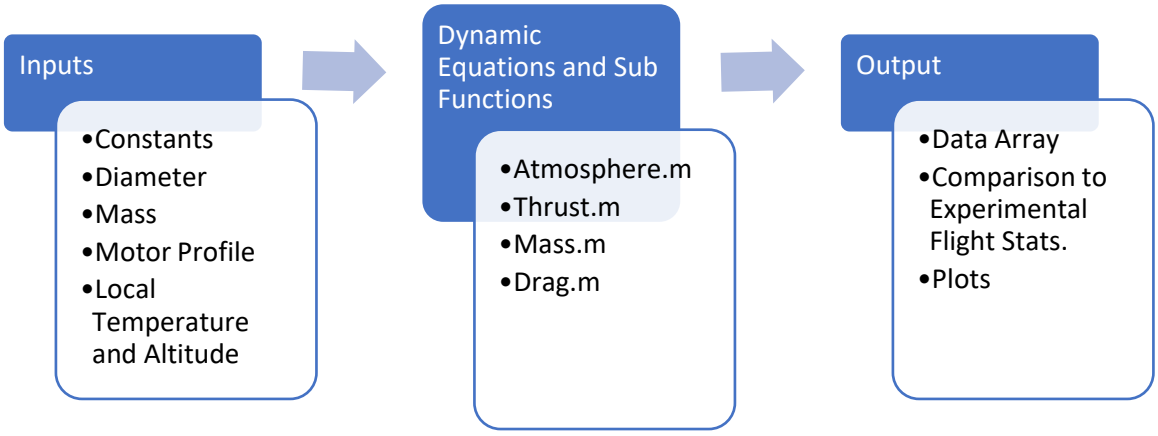

Figure 31: *Flowchart of the operations in Basic_Rocket_Sim.m.*

The simulation uses a mathematical model subject to the following assumptions:

1. Flat earth which does not move relative to the rocket or atmosphere.
2. The rocket is a rigid body.
3. The atmosphere is at rest and the rocket does not experience perturbation.

Given these assumptions, the basic forces on the rocket are described in Figure (32) and equation (5) in inertial coordinates representing the horizontal and vertical axis.

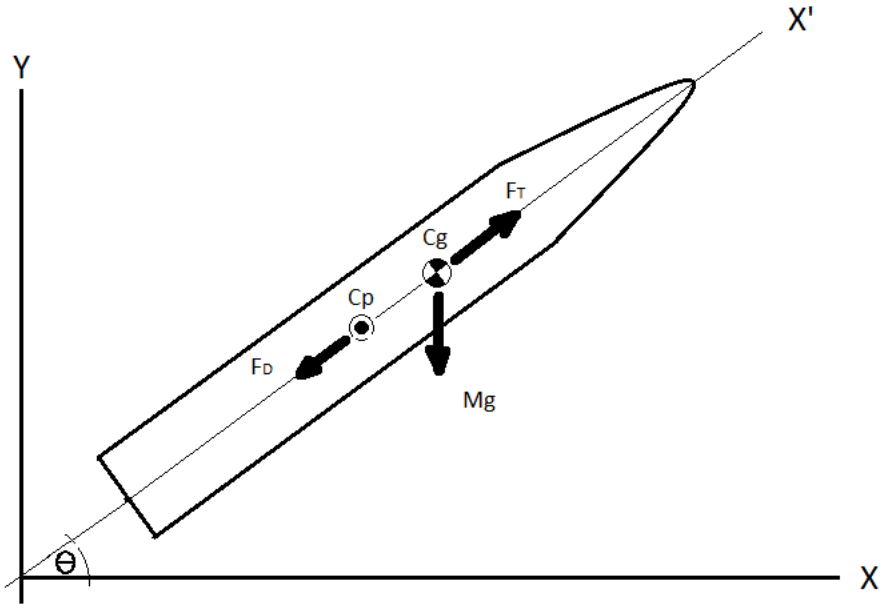

Figure 32: *The basic forces on the rocket represented in Equations (5) & (6).*

$$\rightarrow^{+} \ \Sigma F_x = M\ddot{X} = F_T \cos\theta - F_D \cos\theta \tag{5}$$

$$\uparrow^{+} \ \Sigma F_y = M\ddot{Y} = F_T \sin\theta - F_D \sin\theta - Mg \tag{6}$$

Where:

M = Mass [kg]

F_T = Force of Thrust [N]

F_D = Force of Drag [N]

g = Gravitational Acceleration [N]

θ = Angle of the symmetrical axis from the horizontal

The main body of the program numerically calculates the velocities and positions for each axis from equations (5) & (6) using Euler Integration with a given time step. As the resolution of the time step increases, so does the accuracy of the solution. In order to model the simulation in accordance with a real launch scenario, the program uses conditionals to

evaluate three phases of calculations. The first phase models the rocket as it dwells on the pad while being restrained by a launch rail until it reaches a positive vertical acceleration. The second phase models the fixed trajectory while accelerating on the rail of given length and angle from the horizontal. The third and final phase is the unconstrained acceleration and motion of the rocket off of the rail.

With each iteration, four sub-functions are used to determine the mass, aerodynamic force, thrust and properties of the Standard Atmosphere. The sub-function, Mass.m, uses equation (7) to determine the mass of a rocket with a solid propellant motor at each time step [1].

$$M = m_0 - \frac{m_p}{t_p} * t \tag{7}$$

Where:

M = Mass [kg]

m_0 = Initial mass of the vehicle [kg]

m_p = Mass of the propellant [N]

t_p =Burn duration [s]

t = Instantaneous time [s]

The sub-function, Thrust.m, determines the thrust force at each time step from a given thrust curve. In model rocketry, a profile of the engine is often available from sellers on the web as shown in figure (33). This particular motor, M1400, powered the Dark Star rocket.

Motor:	Cesaroni M1400
Contributor:	Casey Hatch
Submitted:	May 30, 2006
Last Updated:	May 30, 2006
Data Format:	RASP
Data Source:	Manufacturer
License:	Unknown

Statistics	Declared	Calculated	Official
Diameter (mm):	75.0	n/a	75.0
Length (cm):	75.7	n/a	75.7
Prop. Weight (g):	2,992.0	n/a	2,992.0
Total Weight (g):	5,302.0	n/a	5,302.0
Avg. Thrust (N):	—	1,405.2	1,398.0
Max. Thrust (N):	—	2,291.8	2,291.8
Tot. Impulse (Ns):	—	6,251.5	6,251.0
Burn Time (s):	—	4.4	4.5

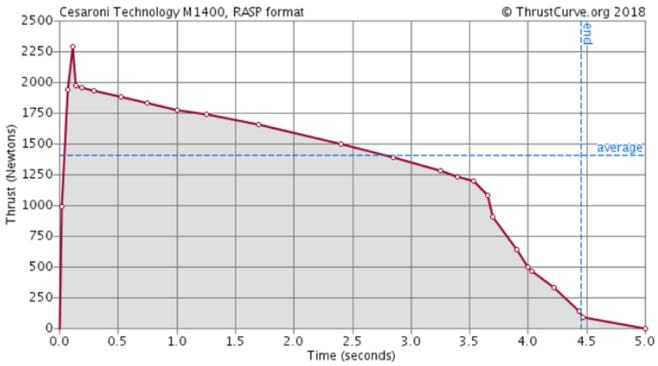

Figure 33: *Motor profile from http://www.thrustcurve.org/simfilesearch.jsp?id=332.*

This information included a data set that was used to construct multiple spline lines and their equations over distinct intervals in Excel. These equations were included in the sub-function, Mass.m, to calculate the force of thrust at each time step within the appropriate interval. The thrust curve, propellant mass, and burn duration represent the motor profile. This information is a required input to "fly" a mass in the simulation.

The properties of the atmosphere at a discreet altitude up to 11 km, are calculated using the Atmosphere.m sub-function. Equations (8) –(12) are used to evaluate pressure, density, and temperature from a launch altitude and its ambient temperature based on the 1976 Standard Atmosphere model and the ideal gas law [2]. Local altitude and air temperature are considered in the calculation.

$$p = p_0 \left(1 + \frac{T_h}{T_0} * h\right)^{\frac{-g}{R * T_h}} \tag{8}$$

$$\rho = \frac{p}{RT} \tag{9}$$

$$T = T_0 \left(1 + \frac{T_h}{T_0} * h\right) \tag{10}$$

$$T_0 = T_L - h_L * T_h \tag{11}$$

$$h = h_R - h_L \tag{12}$$

Where:

$p = Pressure\ [Pa]$

$\rho = Density\ \left[\frac{kg}{m^3}\right]$

$T = Temperature\ [K]$

$T_h = Gradient\ of\ Temperature\ (0\ km < h > 11km) = -6.5 * 10^{-3}\ \left[\frac{K}{m}\right]$

$g = 9.801\ \left[\frac{m}{s}\right]$

$R = 287\ \left[\frac{J}{kg*K}\right]$

$p_0 = 101{,}325\ [Pa]$

$h = Altitude\ [m]$

$h_L = Launch\ Altitude\ [m]$

$h_R = Instantaneous\ vertical\ displacement\ of\ the\ rocket\ [m]$

The sub-function, Drag.m, uses Mach number intervals to calculate the coefficient of drag, C_D. From equations (5) and (6) the force of drag is demonstrated by equation (13).

$$F_D = \frac{C_D}{2}\rho A_r U^2 \tag{13}$$

Where:

$C_D = Coefficient\ of\ Drag$

$\rho = Density\ \left[\frac{kg}{m^3}\right]\ at\ a\ discreet\ altitude$

$A_r = Reference\ area\ [m^2]$

$$U = Velocity\ in\ the\ flight\ direction\ \left[\frac{m}{s^2}\right]$$

The C_D is modeled as a constant value on the interval [0, .8]. From Mach .8 to 1.2 a curve fit represents the Mach rise determined from the Dark Star data. The fit, data points and calculated Mach numbers used in the simulation are shown in figure (34).

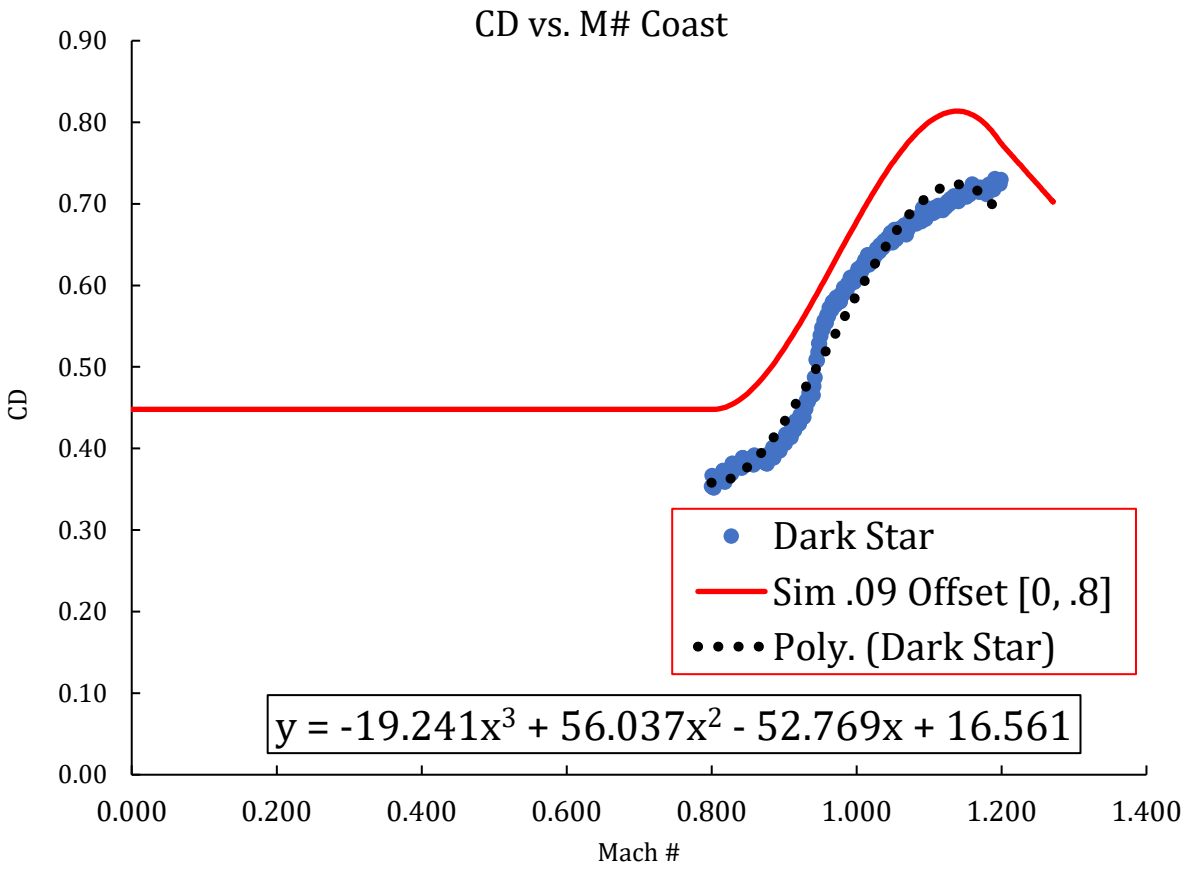

Figure 34: *The fit, data points and calculated Mach numbers used in the simulation are shown. The Mach rise was evaluated by using the polynomial fit equation (above) on the Mach interval [.8, 1.2] and was translated by a value of (.09) when calculated in the simulation.*

$C_D = (.45)$ is constant for all Mach numbers below (.8). The Mach rise starts at $C_D = (.45)$ and reaches a maximum value of (.81). For the purpose of this calculation, the

unpowered phase was examined. The data from the Dark Star rocket was chosen after a nominal burn duration of 4.4 s from Mach [.8, .12] so as to eliminate the error induced by approximating the force of thrust. The equation for determining the C_D was reduced to equation (14) in the rocket's coordinate system with the symmetric axis, x', from figure (32) as the primary axis. The angle θ describes the flight direction from the horizontal.

$$C_D = -2 \times M \frac{(\ddot{x}_r + g \sin\theta)}{\rho A_r U^2} \tag{14}$$

Some iteration was required to establish the (.09) offset, effectively, raising the upper and lower bounds of the Mach rise. One method was to examine the velocity, U, vs. the vertical acceleration from flight and simulated data as shown in figure (35).

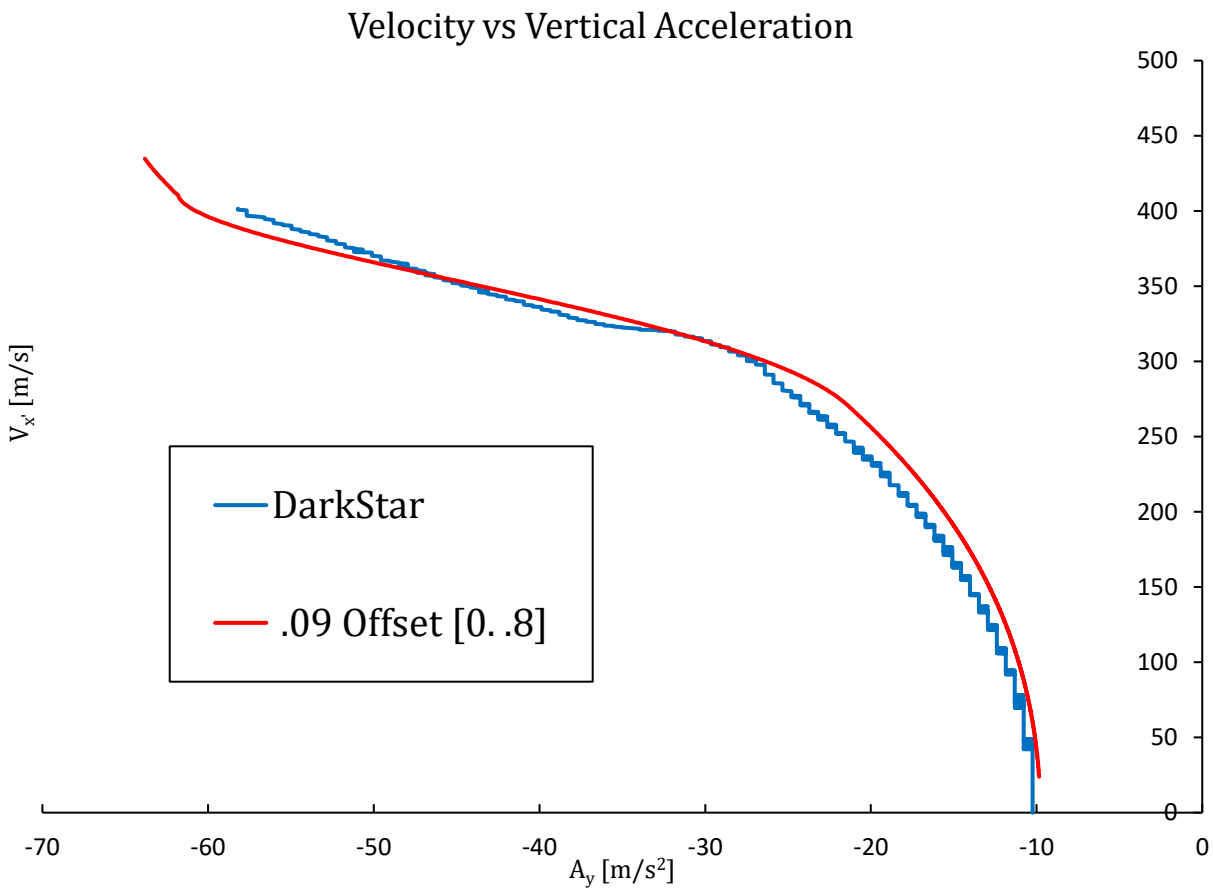

Figure 35: *The velocity vs. vertical acceleration graph was used to translate the polynomial fit equation in order to refine the approximated* C_D.

The schedules for vertical acceleration, velocity, and displacement from the flight data were compared to those of the simulation over the same time interval, 28.68 s, at the same resolution, .01 s. The data generated from the simulation, Coast.m, used the values from the first time step of flight data as initial conditions for the ensuing Euler integration. The comparative schedules are shown in figures (36), (38), (39), and (40).

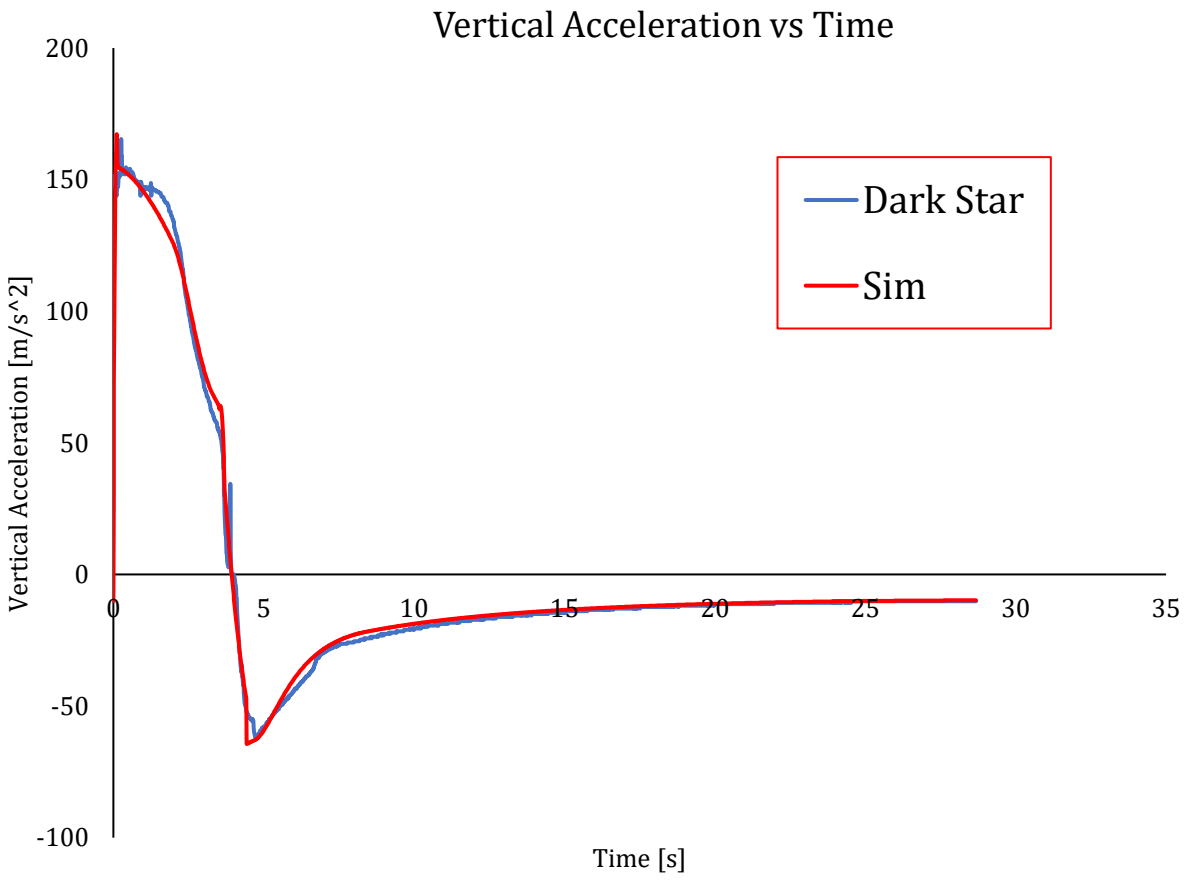

Figure 36: *The vertical acceleration vs. time comparison with an adjusted peak from the thrust profile.*

The two peak accelerations for the flight and simulated data are 165.4 $\frac{m}{s^2}$ and 167.3 $\frac{m}{s^2}$, respectively, which results in a 1.1% error. The nominal thrust curve for the M1400 motor exhibited a peak thrust of 2291.75 N which is not seen in the flight data. The force of thrust dominates in equation (6) between 0 s and .14 s which is where the spike occurs. F_D << F_T , 5 N and 2291.75 N, respectively, during this time period. With an accurate mass and gravitational constant, the peak thrust was adjusted accordingly to reflect the empirical results. The nominal thrust curve was adjusted to 97%, as well, with the knowledge that the information given by the manufacturer has an error of $\pm$ 5%. Figure (37) shows the adjusted calculation to nominal.

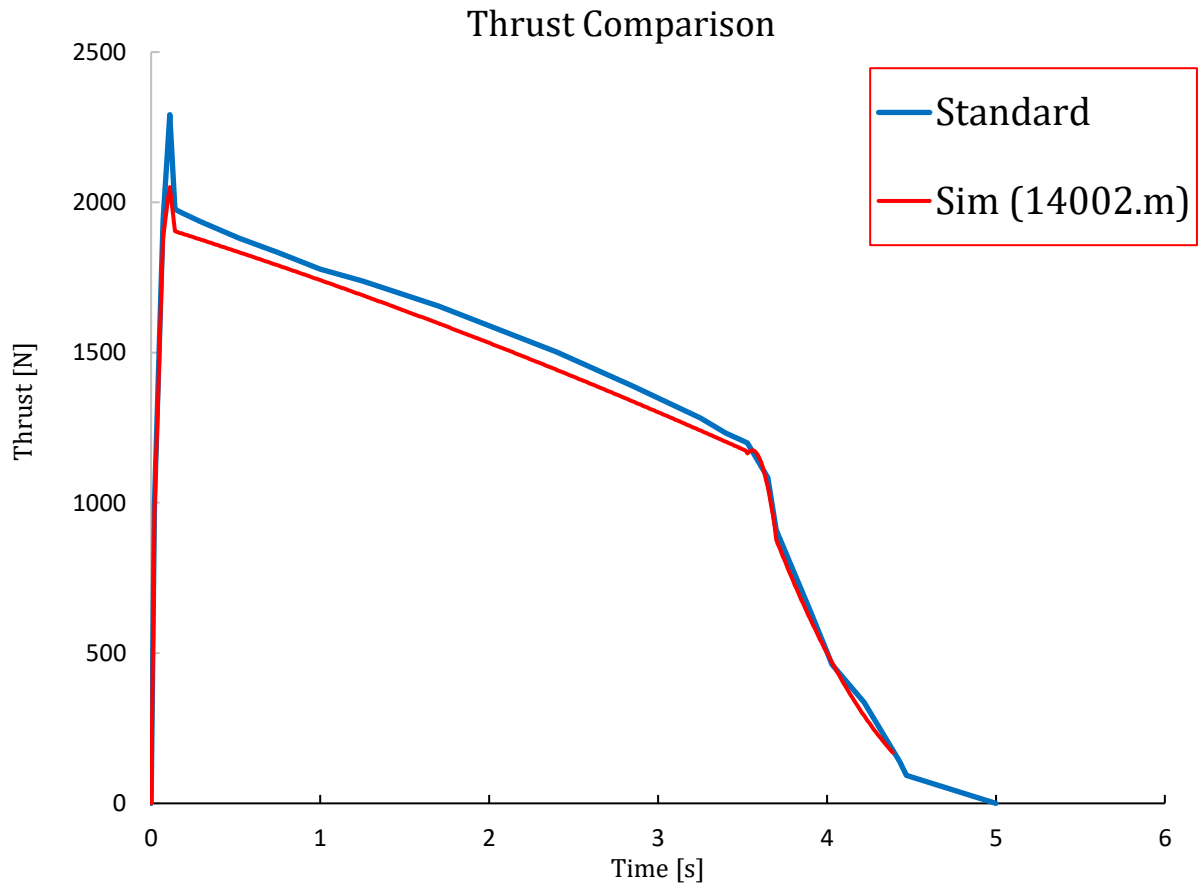

Figure 37: *Thrust comparison between nominal and adjusted calculations within the simulation. These adjustments reflect a process utilized for iterative flights of the same configuration.*

Figure (38) shows the velocity vs time schedules. The two peak velocities for the flight and simulated data are 445.3 $\left[\frac{m}{s}\right]$ and 437.8 $\left[\frac{m}{s}\right]$, respectively, which results in a 1.7% error.

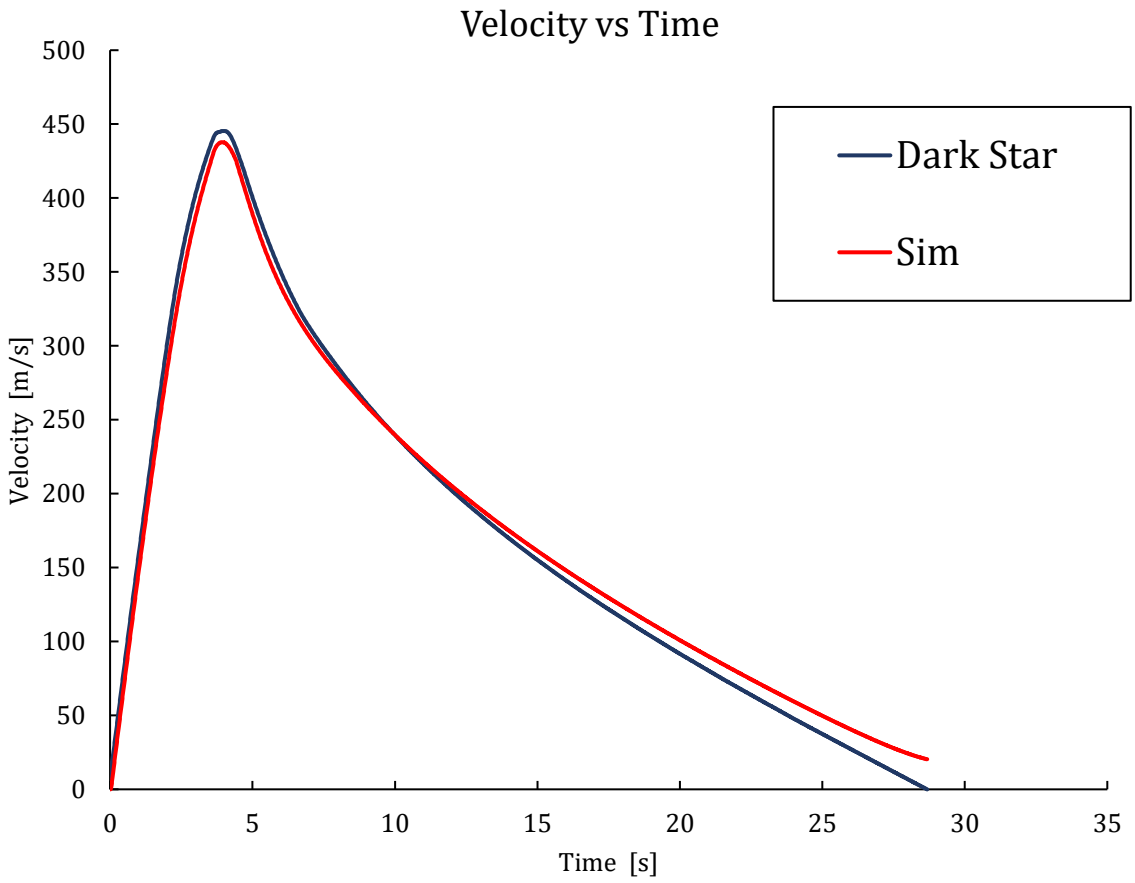

Figure 38: *The velocity vs. time comparison. The rocket reaches apogee at 28.6[s] while the simulation takes 29.6 [s] (not shown). Some time-lapse occurs between flight and simulation due to the resolution of the flight computer.*

Figure (39) shows the vertical displacement vs time schedules. The two maximum altitudes for the flight and simulated data are 6607.5 $[m]$ and 6691.5 $[m]$, respectively, which results in a 1.7% error.

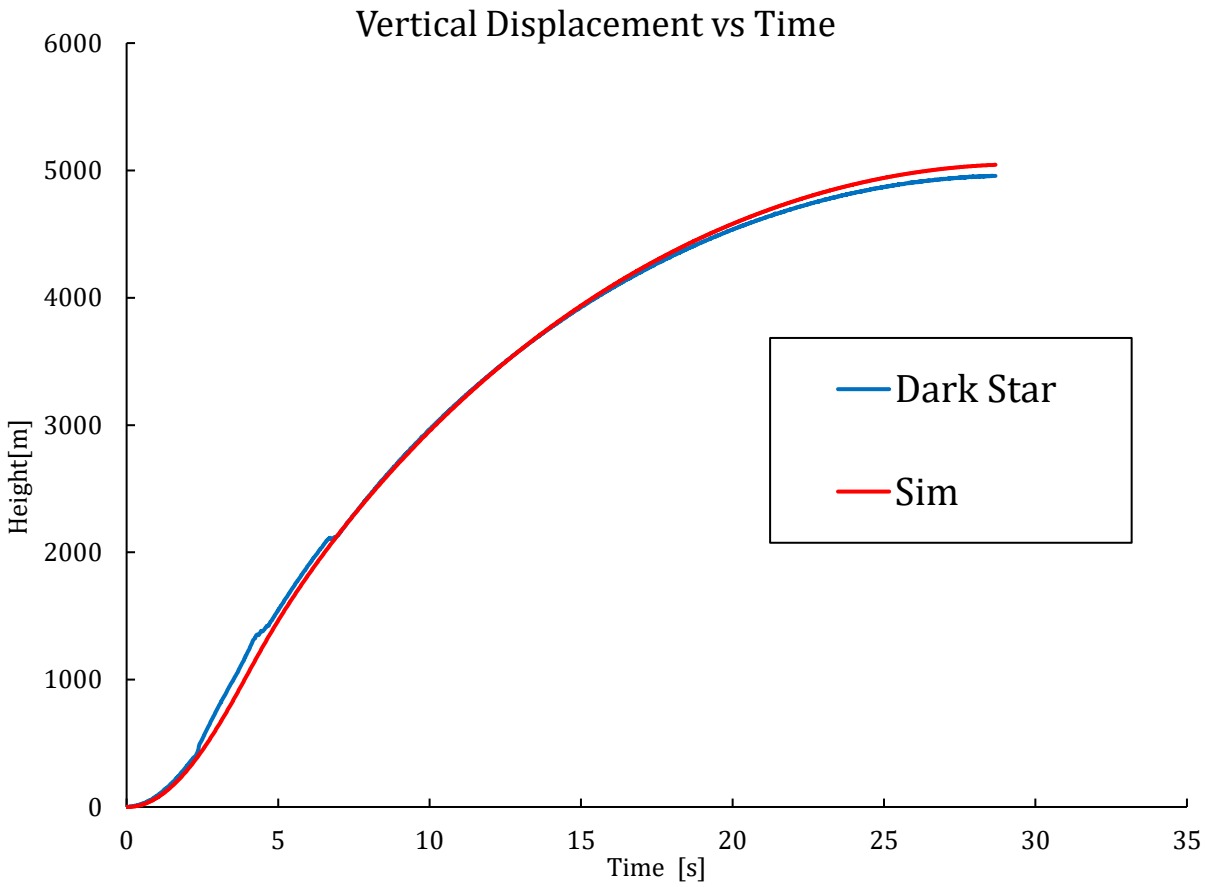

Figure 39: *The Displacement vs. time comparison from a launch altitude of 1642.68 [m]. The rocket reaches apogee at 28.6[s] while the simulation takes 29.6 [s] (not shown). Some time-lapse occurs between flight and simulation due to the resolution of the flight computer.*

Figure (40) shows the angular displacement, θ, vs. time schedules. The rocket undergoes perturbation and develops an angle of attack which induces a lift force. A component of the lift force contributes to the drag force when the axis of symmetry is not

aligned with the direction of the velocity. Since these angles are small and for the purpose of approximating a drag coefficient, their effects are not considered in the calculations.

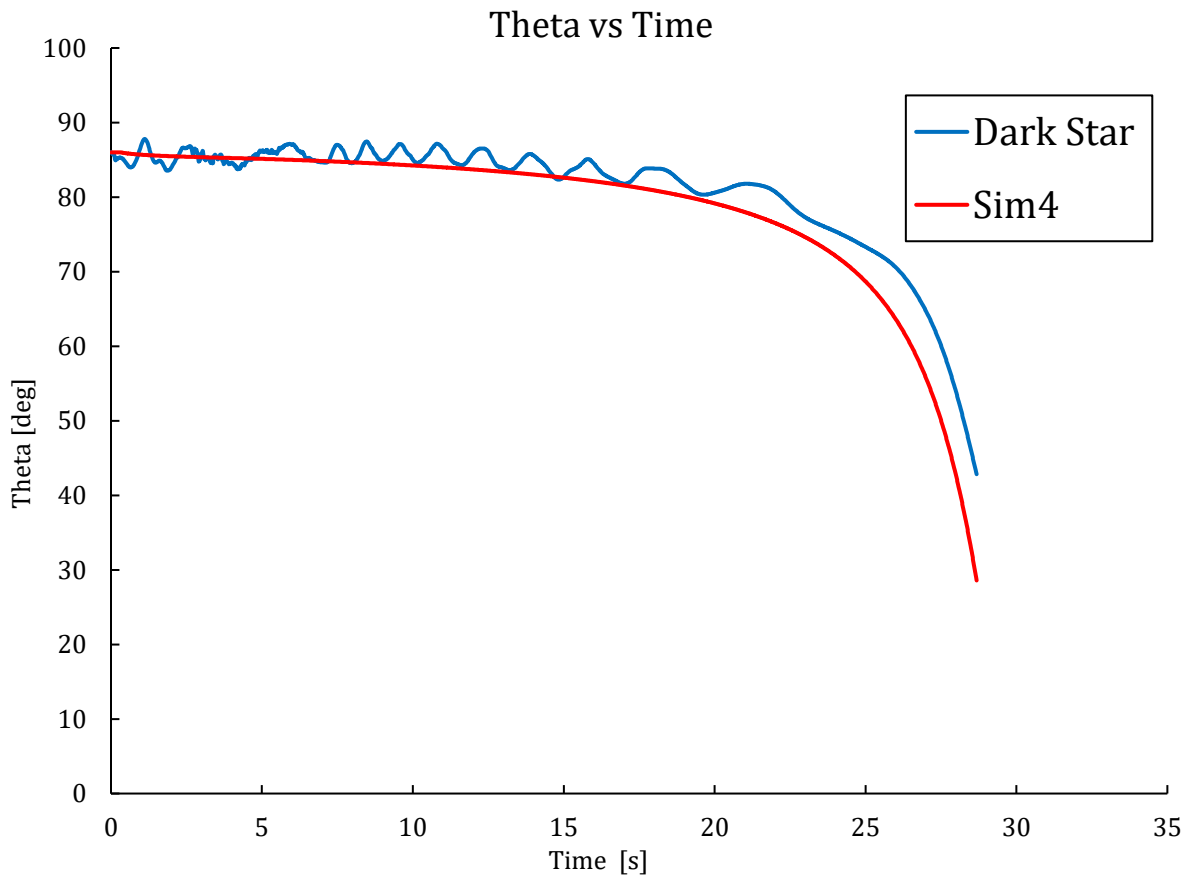

Figure 40: *The angular displacement vs. time comparison. The effects of perturbation are not considered in this basic simulation.*

The simulation proves useful in predicting the flight characteristics of a designed rocket body with a motor profile as shown in table (11).

Table 11: *Flight statistics comparison.*

Statistics	Flight	Simulation	Error [%]
Altitude [m]	6607.5	6691.5	1.3
Speed [m/s]	445.3	437.8	1.7
Vertical Acceleration [m/s^2]	165.4	167.3	1.1

Once the maximum acceleration is calculated, the forces and stresses on the airframe can also be calculated as a function of section height, geometry, and the associated mass properties of the sections being analyzed. A general free body diagram is described in figure (31).

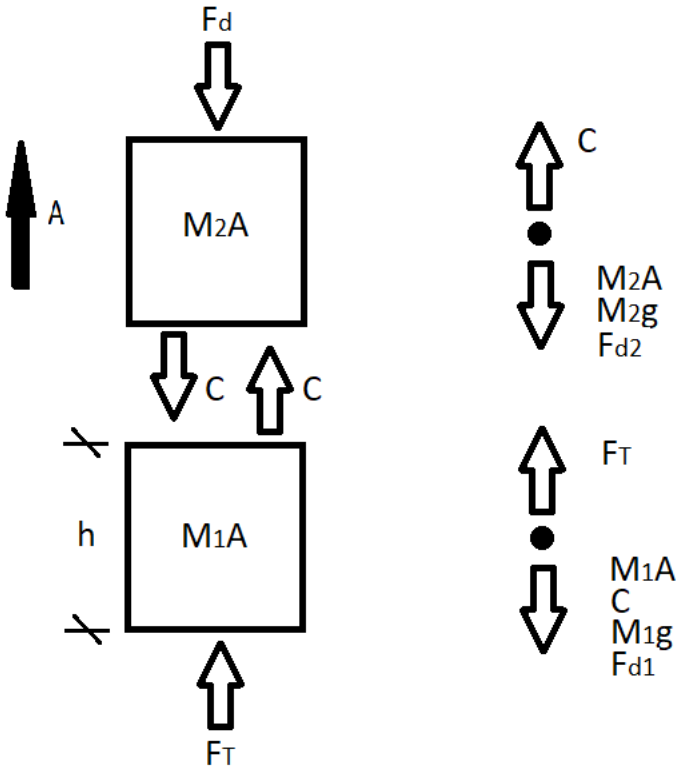

Figure 41: *Free body diagram of forces at a given section height along the symmetrical axis of the rocket.*

Original Simulation Output

TRR 2 .27 C_D Floor (Balls)

Given:

Rocket diameter - 8 inches = 0.2032 meters
Burn time - 11.02 seconds
Propellant mass - 189.723 pounds = 86.06 kg
Mass of casing, closures (no propellant added) - 100 pounds = 45.36 kg
Total mass (without nose cone) - 289.723 pounds = 140.488kg
Total mass (with everything) - 335 pounds = 151.95 kg
I_{sp} =228 s

Results:

For a Length to diameter ratio of: 5

Thickness calculated: th = 0.804 [mm] = 0.032 [inches]

Area calculated: area = 0.00051 [m^2]

Density of Nose Assy 2600.000 [kg/m^3]

Mass of LVH 5:1 1.730 [kg]

Mass of Shell @ 1 Cal. 0.270 [kg]

Ult Stress =110.000 [MPa]

Max V Stress at LVH base =8.586 [MPa] SF @Max Velocity 12.8

Max A Stress at LVH base =8.586 [MPa] SF @Max Acceleration 12.8

Max A Stress at Shell =11.587 [MPa] SF @Max Acceleration 9.5

Altitude =83410.8 [m] Launched From 579.0 [m]

Speed =1579.0 [m/s]

Vertical Acceleration =195.7 m/s^2

Mach # 5.2

Max Acceleration			
tt	11.021	s	
X	712.1656	m	
Y	7864.422	m	
Vx	147.4	m/s	
Vy	1571.951	m/s	
Ax	-9.11454	m/s^2	
Ay	-107.013	m/s^2	
U	1578.954	m/s	
A	196.65	m/s^2	20.0 g's
Alt	8443.422	m	
M#	5.157251		
ϴ	84.6431	deg	
Mp	0	kg	
F_D	5508.269	N	
F_T	0	N	
C_D	0.273353		
M_R	56.428	kg	
ρ	0.498545	kg/m^3	

Max Velocity		
tt	11.021	s
X	712.1656	m
Y	7864.422	m
Vx	147.4	m/s
Vy	1571.951	m/s
Ax	-9.11454	m/s^2
Ay	-107.013	m/s^2
U	1578.954	m/s
A	196.65	m/s^2
Alt	8443.422	m
M#	5.157251	
ϴ	84.6431	deg
Mp	0	kg
F_D	5508.269	N
F_T	0	N
C_D	0.273353	
M_R	56.428	kg
ρ	0.498545	kg/m^3

Figure 42: *Max Acceleration and Max Velocity calculations from simulation.*

Table 12: *Calculations and program inputs.*

Calculations					
I_{SP}=	228.8154	s	Calc Mp=	86.10305	kg
g_0=	9.80665	m/s^2	Calc Impulse=	193207.7	N*s
c=	2243.912	m/s	Mass Ratio=	2.525129	
			Max ΔU no g ,F_D=	2078.519	m/s
			Max Disp. Powered No F_D=	9113.873	m
			Avg Ft=	17532.46	
Program Inputs					
Added Mass (mX)=	2	kg			
Mp=	86.06	kg			
M_0=	140.488	kg			
M_f=	56.428	kg			
tp=	11.02	s			

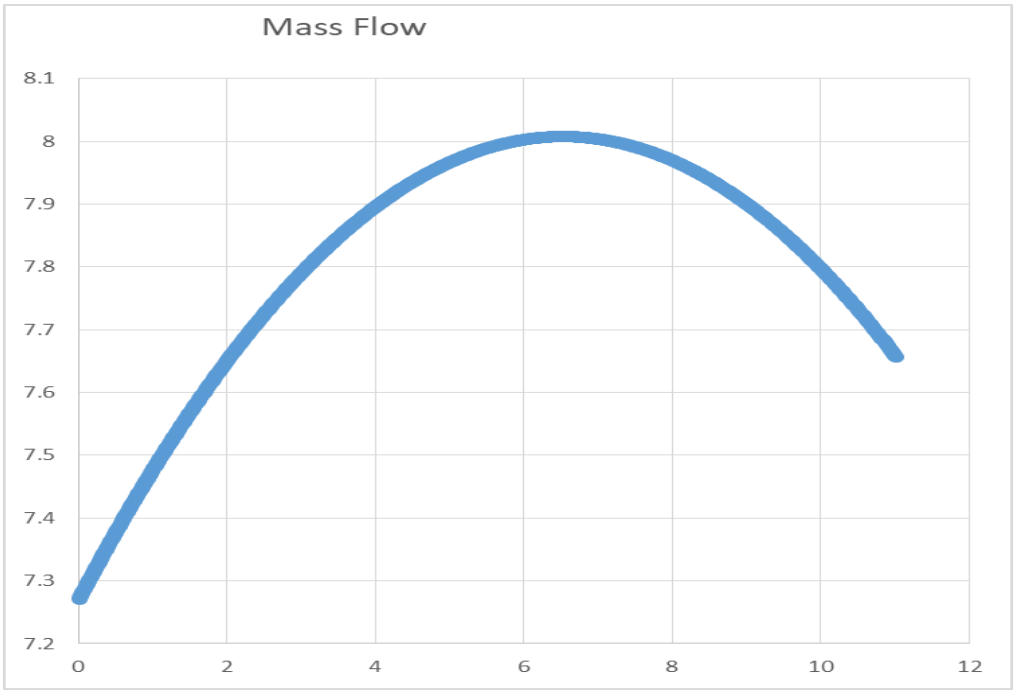

Figure 43: *Mass flow over time to be checked with thrust curve.*

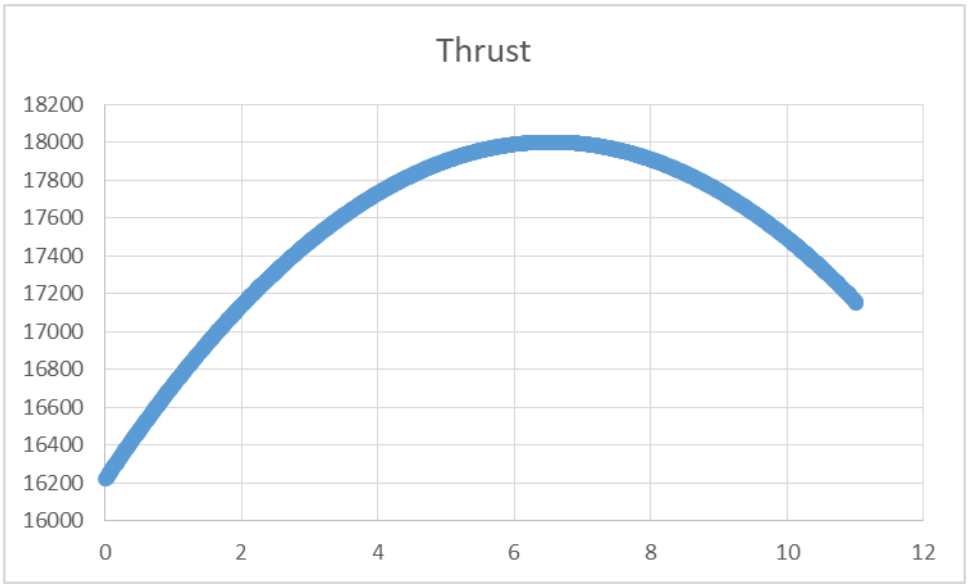

Figure 44: *Thrust curve over time to be checked with the mass flow curve.*

The thrust curve is proportional to the mass flow curve. Specific impulse and propellant mass are congruent with the given data. Maximum velocity in the simulation, 1579.0 [m/s] is within the theoretical threshold of the maximum velocity increment in a gravitation less and drag free space, 2078.5 [m/s]. The powered displacement in the sim at

the end of burn time, 11.02 [s], is 7862.8 [m] which is less than the theoretical displacement of 9113.8 [m] in a drag free space. The mass of a one caliber shell and LVH 5:1 have to be verified. It is recommended to proceed with the production of the nose assembly parts beyond the calculated thickness and to fabricate a thickness 'that works' as that mass will not be a significant factor.

Program Architecture

For the mass properties and inertia calculations, the densities are to be determined, however, will be set to average values for aluminum and fiber glass, 0.10 [lb./in.^3] and 0.05 [lb./in.^3] respectively. For the rocket profile desired, there are three geometries used: Cylindrical shells, Barrowman fins, and LV-Haack nose cone. The cylindrical shell method takes the rocket's governing outer-diameter and a specified wall thickness to revolve the profile to obtain a volume and mass. These shells can be simply added as needed using the programmed cylindrical shells function file. The Barrowman Fin profile is defined by four parameters, fin-root chord, fin-tip chord, fin semi-span, and midpoint distance. Once the profile has been defined the desired thickness is used to output volume and mass. After one fin is output, the program also takes n number of fins and generates a symmetrical array around the fin-can. The LV-Haack file is much more involved as its cross-sectional area is not constant along its length. The LV-Haack nose cone file takes a diameter-to-length ratio as parameter and solves for the varying radius that corresponding to a location x along the nose cone.

$$\theta = \cos^{-1}\left(1 - \frac{2x}{L}\right) \tag{15.a}$$

$$y = \frac{R}{\sqrt{\pi}} \times \sqrt{\theta - \frac{\sin(2\theta)}{2} + C\sin^3(\theta)} \quad (15.b)$$

Where y is the varied radius, and R represents the maximum radius at the base of the nose cone. L represents the desired length of the nose cone. C is a parameter that defines the shape of the nose cone, where $C = \frac{1}{3}$ has a more tangential fit with the body tube of the rocket. Using the governing LV-Haack equations, this file can take a maximum allowed mass to obtain a calculated optimum wall thickness to meet the design specifications. Once the thickness has been solved for, the inner-diameter of the nose cone is solved for by taking the anti-normal surface unit vector at each point along the outer diameter and is scaled by the magnitude of wall thickness. A point is plotted at the tip of each vector along the length of the nose cone. Once the plot of points for the inner diameter is solved, a seventh-order polynomial fit is applied to generate a function that will be used to integrate using a volume by shells method.

Additionally, beyond the mass and volume outputs, the center of mass at each component is being calculated using the center point of the nozzle as datum, with the positive direction of x-axis pointing to the forward end of the rocket. The y- and z-axes are co-planar with the aft end of the rocket. The coordinate system is currently a work in progress and will be programmed to be in agreeance with the material properties software.

Results

The dimensions that will be used are to be determined, however, a guessed solution has been used to test the functionality of the software.

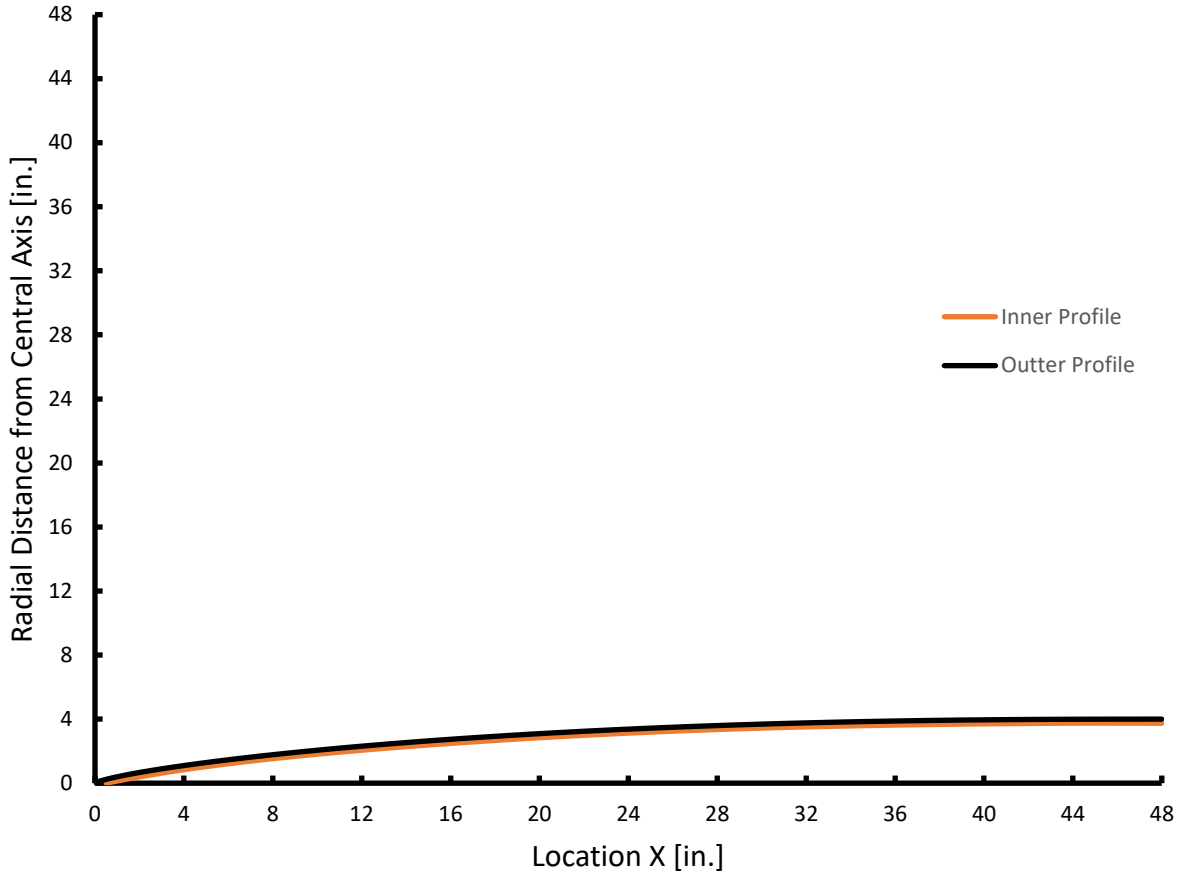

Figure 45: *LV-Haack profile with X-axis of symmetry.*

The aspect ratio must be maintained as a 1:1 to accurately display the shape of the cone. Figure 1 displays the full profile of the cone, to which was revolved around the x-axis to obtain the geometries that fit the maximum mass allocated. For a closer view of the detail, and accuracy of the approximated inner diameter a zoomed profile can be seen.

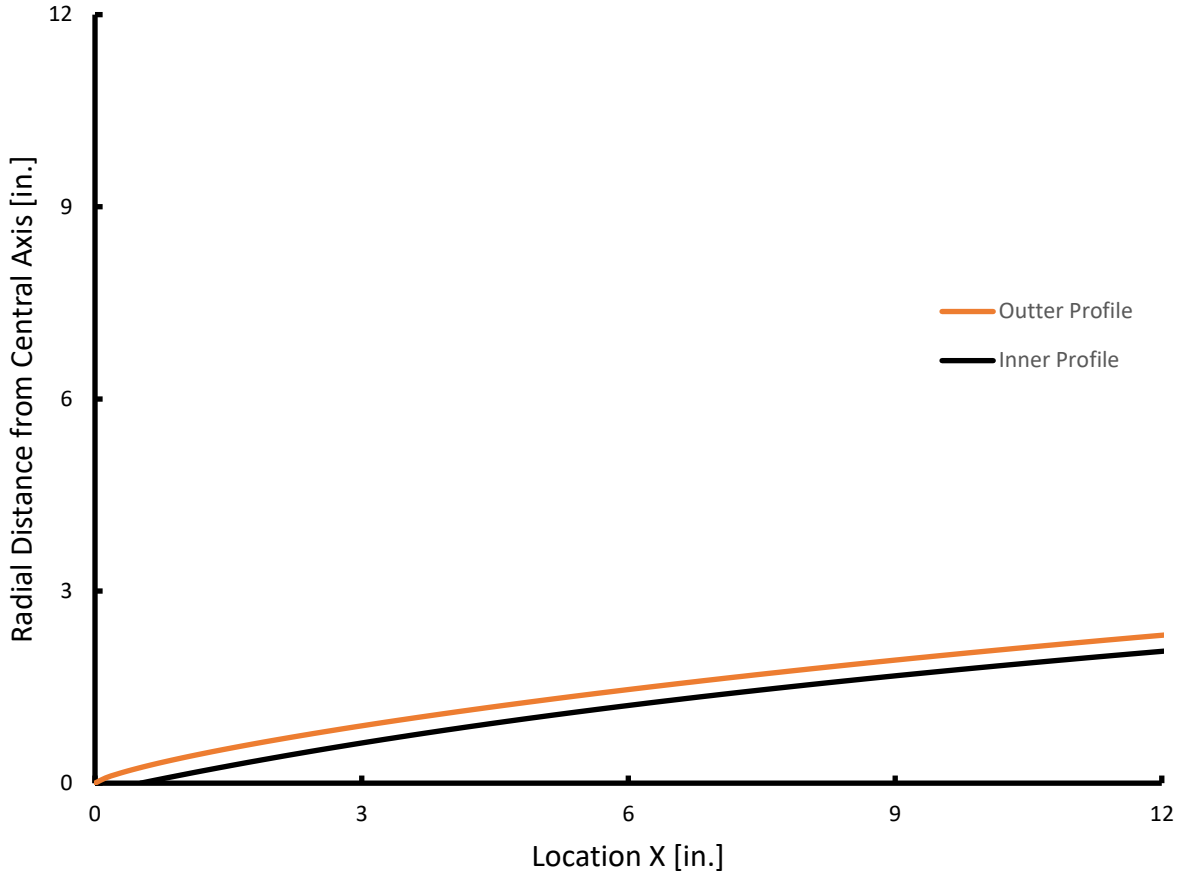

Figure 46: *Zoomed View of the LV-Haack profile with X-axis of symmetry.*

The forward end of the nose cone resulted in the most amount of error. The error in constant thickness tends to zero as x approaches the length of the rocket.

Density = 0.00 grams per cubic millimeter

Mass = 6759.62 grams

Volume = 6759621.48 cubic millimeters

Surface area = 1073032.07 square millimeters

Figure 47: *List of mass property results of LV-Haack nose cone as solved by SolidWorks.*

The results shown in figure (47) were calculated by SolidWorks Mass Properties tool. These results can be compared to the value obtained using the MATLAB procedure programmed.

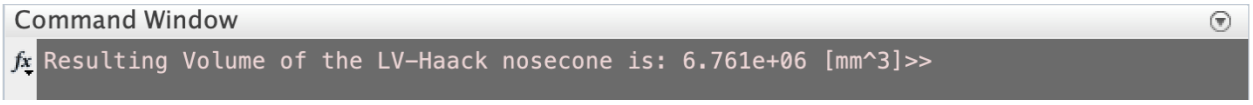

Figure 48: *Resulting volume of LV-Haack nose cone as solved by program.*

The results in figure (47) compare closely to the calculated results shown in figure (48) using the method described in *Materials and Methods* section. The mass properties were compared to SolidWorks models built using the same guessed parameters. The results calculated were less than 1% difference with respect to the values displayed by the SolidWorks measurements tool.

Discussion of Program

The mass properties for the shell and fin sections of the rocket can be treated as exact calculations since those geometries are well known. As for the LV-Haack profile, these calculations are only approximate within 1% accuracy due to their complexity. The error towards the forward end of the nose cone could be result of calculating the positive root of the polynomial fit used to define inside of the shape. MATLAB's fzero command was used to solve for the polynomial's root, using a guess of 0.02 [in.] along the length of the nose cone. The fzero routine iterates until a stop condition was met, for this case, an error less than 10 millionths. Once the root was solved, an array was created using this offset value as the first index of x.

The design method is tentative and has since changed since the start of the project. Initially the program was first calibrated in order to test the accuracy of calculations. Once the calculations are properly calibrated, the design architecture and functionality will be implemented. The program does have a goal, which is to match a cross-sectional area of the base of the nose cone to the area in the stress calculation along with a clever safety factor.

Pressure Transducer

An analog pressure transducer will be used to measure the change of pressure over a change in time. This data will be used to optimize the amount of black powder charge that will be used to eject the nose cone and initiate recovery. To do so, a 1600 [psi] pressure transducer was used. The device is an analog ratiometric sensor with a 5 [Vdc] input with a max output of 4.5 [Vdc]. The sensor divides the maximum specified rating of 1600 [psi] into a 10-bit resolution. The sensor will be powered by an Arduino UNO Rev3 microcontroller and an analog pin will read the signal wire. To obtain the gage pressure the sensor detects, the bits read from the signal wire will be multiplied by a conversion factor with units of [psi/bit]. Refer to Arduino code in the appendix for the conversion method.

When the device is first running and ready to collect data the program takes the average pressure reading over the first half second of being activated. The average pressure that is obtained and calculated will act as a way to zero the device to read a gage pressure. The frequency of the data collection is approximately 1000 [Hz]. The results will be printed to the serial monitor which can then be imported into MATLAB and converted into an array.

Discussion of Code

The devices maximum specification of 1600 [psi] too high since it is a ratiometric device and will be incremented by 10-bits regardless of the voltage input. The pressure step

is 2.0 [psi] rounding to the nearest tenth which is too coarse for the data desired. To achieve better resolution a lower specification is of interest.

Conclusion

Having the opportunity to launch a rocket at BALLS 28 was a huge accomplishment for us. It allowed us to nail down our design and test our skills of mixing a large motor. We modified the things that we wanted to change and worked towards our goal of building a large rocket for a high-altitude attempt, but then had to change the design due to budgetary restrictions. We modified and made a new propellant, changed the design for the forward closure/adapter to the nose cone, and did more analysis on every part we made either through flow simulation, finite element analysis, or hand calculations. We are excited for the day that we get to launch this rocket.

References

[1] Sutton, George P. , Biblarz, Oscar: *Rocket Propulsion Elements : an introduction to the engineering of rockets*. New York: John Wiley & Sons, Inc., 7th ed. 2001. Print.

[2] Boiffier, Jean-Luc. *The Dynamics of Flight : The Equations.* New York: John Wiley & Sons, Inc., 1998. Print.

[3] Parker Hannifin Corporation. *Parker O-Ring Handbook ORD 5700*. 2018. CH 4. Web.

Appendices

Rocket Basic Sim MATLAB Code

```
%Rocket_Basic_sim1
clc
clear
close all
%      Constants
dt=.01;% [s] time step
m0=11.61;% [kg] Initial total mass of rocket
mp=2.992;% [kg] Mass of Propellent
tp=4.4;% [sec] Burn time
Dia=.102;%[m] Max diameter of rocket body
Ar=pi()/4*Dia^2;% [m^2]Ref. Area
YL=1642.68;% [m] Local Altitude
TL=28.7;% [C] Local Temp
RailLength=6.5;%[m]6.5
g=9.81;%[m/s^2]
ta=28.68;%Time to apogee from flight data (Approx)
psi0=86*pi()/180;% [radians] Initial Flight direction from horizontal
maxit=1000000;%maximum Iterations
%      Preallocate Arrays
dat = zeros(17,maxit);
Stat=zeros(15,1);
Err=zeros(3,1);
Boostexport=zeros(1,6);
%Initialize Variables
m=m0;
z1=0;z2=0;%Initial Pos X,Y
z3=0;z4=0;%Initial Velocities X,Y
Ay=0;Ax=0;%Initial Accel X,Y
Cd=0;
Fd=0;
Mprev=0;
for i=1:maxit
   tt=(i-1)*dt;
   A=(Ax^2+Ay^2)^(1/2);
```

```
V=(z3^2+z4^2)^(1/2);
Yr=z2;% Hieght of Rocket
%Standard Atmosphere Calc with Offset
[M,Row,P,T,Y]=Atmosphere(YL,Yr,TL,V);

[Cd]=Drag_Forensic1(M);%Dragconst;
k=Cd/2*Row*Ar;
[Ft]=m14002(tt);% Thrust Curve of Motor
%2nd Law Euler Integration
% Rocket Dwells on the lauchpad
if Ay<=0 & tt<tp & z2/sin(psi0)<=RailLength
   Ff=.6*cos(psi0)*m*g;%Rail friction
   Ax=1/m*(Ft*cos(psi0)-cos(psi0)*Ff);
   Ay=1/m*(Ft*sin(psi0)-m*g-sin(psi0)*Ff);
   z1=0;
   z2=0;
   z3=0;
   z4=0;
   Theta=psi0*180/(pi());
 %Rocket launches on rail
 elseif Ay>=0 & z2/sin(psi0)<=RailLength & tt<tp
   Ff=.2*cos(psi0)*m*g;
   Ay=1/m*(Ft*sin(psi0)-k*V^2*sin(psi0)-m*g-sin(psi0)*Ff);
   Ax=Ay/tan(psi0);
   z1=z1+(dt*z3);
   z2=z2+(dt*z4);
   z3=z3+dt*Ax;
   z4=z4+dt*Ay;
   Theta=psi0*180/(pi());
 else% Rocket off the rail
   Ax=1/m*(Ft*z3/(z3^2+z4^2)^(1/2)-
k*abs((z3^2+z4^2)^(1/2))*z3);
   Ay=1/m*(Ft*z4/(z3^2+z4^2)^(1/2)-k*abs((z3^2+z4^2)^(1/2))*z4-
m*g);
   z1=z1+(dt*z3);
   z2=z2+(dt*z4);
```

```
    z3=z3+dt*Ax;
    z4=z4+dt*Ay;
    Theta=atan2(z4,z3)*180/(pi());

Fd=((k*abs((z3^2+z4^2)^(1/2))*z3)^2+(k*abs((z3^2+z4^2)^(1/2))...
    *z4)^2)^(1/2);
  end
   %debug
% dat=dat(1:13,1:(i-1));%Truncates data matrix for plotting
%       break;end

  [m]=Mass(mp,tp,m0,tt);% Mass Function for Solid Prop.
  %Store Data
  dat(1,i)=tt;%time
  dat(2,i)=z1;%x pos
  dat(3,i)=z2;%y pos
  dat(4,i)=z3;%x vel
  dat(5,i)=z4;%y vel
  dat(6,i)=Ax;%x accel
  dat(7,i)=Ay;%y accel
  dat(8,i)=V;% resultant vel
  dat(9,i)=A;% resultant accel
  dat(10,i)=Y;% Altitude
  dat(11,i)=M;% Mach#
  dat(12,i)=Theta;%[Degrees] Flight Angle
  dat(13,i)=m;% mass
  dat(14,i)=Yr;% hieght
  dat(15,i)=Fd;% Drag Force
  dat(16,i)=Ft;% Thrust Force
  dat(17,i)=Cd;% Coefficient of Drag
  %Drag vs Mach Data Plot
  if M>=Mprev
     DragForce(1,i)=dat(11,i);
     DragForce(2,i)=dat(15,i);
     Dcoeff(1,i)=dat(11,i);
     Dcoeff(2,i)=dat(17,i);
```

```
    Mprev=M;
  end

  %Stores selected Data at the end of burn [T,Yacc,ht,Vres,Ares,Theata]
  if  tt<=tp
      Boost=[dat(:,i)];
      Boosttrans=Boost.';
      Boostexport=[Boosttrans(1,1) Boosttrans(1,7) Boosttrans(1,14)...
      Boosttrans(1,8) Boosttrans(1,9) Boosttrans(1,12)];
  end
  %exports Data for schedules
   if tt==ta
      dattrans=dat(1:17,1:i).';
      datexport=[dattrans(:,1) dattrans(:,7) dattrans(:,3) ...
      dattrans(:,8)  dattrans(:,12)];
      xlswrite('Sim_Export', datexport);
   end
  %Rocket hits the ground
  if z2<=0 & tt>tp
    dat=dat(1:17,1:i);%Truncates data matrix for plotting
     break
  end
end
%Exports Cd Data
Dcoefftrans=[Dcoeff(1,:);Dcoeff(2,:)].';
xlswrite('CD_Export', Dcoefftrans);
% max flight statistics [alt(m);speed(m/s);accel(m/s^2);Mach#]
FlightStat=[6607.48;445.3;165.4;1.3];
Stat= max(dat,[],2);% Retrieves max values of each row in the dat[]
MaxAccRes=Stat(9,1); %Max Acceleration along rocket axis
[I,J] = find(dat== MaxAccRes);% Finds the subscript
MaxAccResDat=dat(:,J);% Column vector of data for max resultant accel
%Calculate Error Percentage
Err=[abs(FlightStat(1,1)-Stat(10,1))/FlightStat(1,1)*100;%altitude
     abs(FlightStat(2,1)-Stat(8,1))/FlightStat(2,1)*100;%speed
     abs(FlightStat(3,1)-Stat(7,1))/FlightStat(3,1)*100;%vert accel
```

```
    abs(FlightStat(4,1)-Stat(11,1))/FlightStat(4,1)*100];%Mach #
fprintf('Altitude\n');
fprintf( 'Flight %3.1f m\t',FlightStat(1,1));
fprintf( 'Calculated %3.1f m\t',Stat(10,1));
fprintf( 'Percentage Error %3.1f \n',Err(1,1));
fprintf('Speed\n');
fprintf( 'Flight %3.1f m/s\t',FlightStat(2,1));
fprintf( 'Calculated %3.1f m/s\t',Stat(8,1));
fprintf( 'Percentage Error %3.1f\n',Err(2,1));
fprintf('Vertical Acceleration\n');
fprintf( 'Flight %3.1f m/s^2\t',FlightStat(3,1));
fprintf( 'Calculated %3.1f  m/s^2\t',Stat(7,1));
fprintf( 'Percentage Error %3.1f\n',Err(3,1));
fprintf('Mach #\n');
fprintf( 'Flight %3.1f m/s^2\t',FlightStat(4,1));
fprintf( 'Calculated %3.1f  m/s^2\t',Stat(11,1));
fprintf( 'Percentage Error %3.1f\n',Err(4,1));

figure(1)
plot(dat(1,:),dat(4,:),dat(1,:),dat(5,:))
title('Velocities')
xlabel('Time [s]')
ylabel('Velocity[m/s]')
legend('X','Y')
figure(2)
plot(dat(2,:),dat(3,:))
title('Trajectory')
xlabel('Distance[m]')
ylabel('Height[m]')
figure(3)
plot(dat(1,:),dat(8,:))
title('Velocity')
xlabel('Time [s]')
ylabel('Velocity[m/s]')
figure(4)
plot(dat(1,:),dat(7,:))
```

```
title('Vertical Acceleration')
xlabel('Time [s]')
ylabel('Acceleration[m/s^2]')
figure(5)
plot(dat(1,:),dat(10,:))
title('Altitude vs Time')
xlabel('Time [s]')
ylabel('Altitude[m]')
figure(6)
plot(DragForce(1,:),DragForce(2,:))
title('Drag Force vs Mach #')
xlabel('Mach #')
ylabel('Drag Force [N]')
figure(7)
plot(dat(1,:),dat(14,:))
title('Verical Displacement vs Time')
xlabel('Time [s]')
ylabel('Hieght[m]')
figure(8)
plot(Dcoeff(1,:),Dcoeff(2,:))
title('Cd vs Mach #')
xlabel('Mach #')
ylabel('Cd')
%Coast_sim1
clc
clear
close all
%      Constants
dt=.01;% [s] time step
Dia=.102;%[m] Max diameter of rocket body
Ar=pi()/4*Dia^2;% [m^2]Ref. Area
YL=1642.68;% [m] Local Altitude
TL=28.7;% [C] Local Temp
g=9.81;%[m/s^2]
maxit=1000000;%maximum Iterations
%      Preallocate Arrays
```

```
dat = zeros(17,maxit);
Stat=zeros(15,1);
Err=zeros(3,1);
Boostexport=zeros(1,6);
%Export from Coast Data Initial conditions
maxt=24.28;
Vr=434.74;
tilt=5.53;
Ayr=0;
ht=1367.92;
%Initialize Variables
m=8.618;%Mass empty
psi0=(90-tilt)*pi()/180;% [radians] Initial Flight direction from
horizontal
z1=ht*atan(psi0);z2=ht;%Initial Pos X,Y
z3=Vr*cos(psi0);z4=Vr*sin(psi0);%Initial Velocities X,Y
Ay=0;Ax=0;%Initial Accel X,Y
Cd=0;
Fd=0;
Ft=0;
Mprev=0;
for i=1:maxit
   tt=(i-1)*dt;
   A=(Ax^2+Ay^2)^(1/2);
   V=(z3^2+z4^2)^(1/2);
   Yr=z2;% Hieght of Rocket
   [M,Row,P,T,Y]=Atmosphere(YL,Yr,TL,V);%Standard Atmosphere Calc
with Offset

   [Cd]=Drag_Forensic1(M);
   k=Cd/2*Row*Ar;
   % Rocket off the rail
     Ax=1/m*(Ft*z3/(z3^2+z4^2)^(1/2)-
k*abs((z3^2+z4^2)^(1/2))*z3);
     Ay=1/m*(Ft*z4/(z3^2+z4^2)^(1/2)-k*abs((z3^2+z4^2)^(1/2))*z4-
m*g);
```

```
  z1=z1+(dt*z3);
  z2=z2+(dt*z4);
  z3=z3+dt*Ax;
  z4=z4+dt*Ay;
  Theta=atan2(z4,z3)*180/(pi());
  Fd=((k*abs((z3^2+z4^2)^(1/2))*z3)^2+...
     (k*abs((z3^2+z4^2)^(1/2))*z4)^2)^(1/2);
%Store Data
dat(1,i)=tt;%time
dat(2,i)=z1;%x pos
dat(3,i)=z2;%y pos
dat(4,i)=z3;%x vel
dat(5,i)=z4;%y vel
dat(6,i)=Ax;%x accel
dat(7,i)=Ay;%y accel
dat(8,i)=V;% resultant vel
dat(9,i)=A;% resultant accel
dat(10,i)=Y;% Altitude
dat(11,i)=M;% Mach#
dat(12,i)=Theta;%[Degrees] Flight Angle
dat(13,i)=m;% mass
dat(14,i)=Yr;% hieght
dat(15,i)=Fd;% Drag Force
dat(16,i)=Ft;% Thrust Force
dat(17,i)=Cd;% Coefficient of Drag
%Drag vs Mach Data Plot
if M>=Mprev
   DragForce(1,i)=dat(11,i);
   DragForce(2,i)=dat(15,i);
   Dcoeff(1,i)=dat(11,i);
   Dcoeff(2,i)=dat(17,i);
   Mprev=M;
end
%exports Data for schedules
 if tt==maxt
    dattrans=dat(1:17,1:i).';
```

```
        datexport=[dattrans(:,1) dattrans(:,7) dattrans(:,3)...
           dattrans(:,8)  dattrans(:,12)];
        xlswrite('Coast_Export', datexport);
        break
    end

end
% max flight statistics [alt(m);speed(m/s);accel(m/s^2);Mach#]
FlightStat=[6607.48;445.3;165.4;1.3];
Stat= max(dat,[],2);% Retrieves max values of each row in the dat[]
MaxAccRes=Stat(9,1); %Max Acceleration along rocket axis
[I,J] = find(dat== MaxAccRes);% Finds the subscript
MaxAccResDat=dat(:,J);% Column vector of data for max resultant accel
%Calculate Error Percentage
Err=[abs(FlightStat(1,1)-Stat(10,1))/FlightStat(1,1)*100;%altitude
     abs(FlightStat(2,1)-Stat(8,1))/FlightStat(2,1)*100;%speed
     abs(FlightStat(3,1)-Stat(7,1))/FlightStat(3,1)*100;%vert accel
     abs(FlightStat(4,1)-Stat(11,1))/FlightStat(4,1)*100];%Mach #
fprintf('Altitude\n');
fprintf( 'Flight %3.1f m\t',FlightStat(1,1));
fprintf( 'Calculated %3.1f m\t',Stat(10,1));
fprintf( 'Percentage Error %3.1f \n',Err(1,1));
fprintf('Speed\n');
fprintf( 'Flight %3.1f m/s\t',FlightStat(2,1));
fprintf( 'Calculated %3.1f m/s\t',Stat(8,1));
fprintf( 'Percentage Error %3.1f\n',Err(2,1));
fprintf('Vertical Acceleration\n');
fprintf( 'Flight %3.1f m/s^2\t',FlightStat(3,1));
fprintf( 'Calculated %3.1f  m/s^2\t',Stat(7,1));
fprintf( 'Percentage Error %3.1f\n',Err(3,1));
fprintf('Mach #\n');
fprintf( 'Flight %3.1f m/s^2\t',FlightStat(4,1));
fprintf( 'Calculated %3.1f  m/s^2\t',Stat(11,1));
fprintf( 'Percentage Error %3.1f\n',Err(4,1));

% figure(1)
```

```
% plot(dat(1,:),dat(4,:),dat(1,:),dat(5,:))
% title('Velocities')
% xlabel('Time [s]')
% ylabel('Velocity[m/s]')
% legend('X','Y')
% figure(2)
% plot(dat(2,:),dat(3,:))
% title('Trajectory')
% xlabel('Distance[m]')
% ylabel('Height[m]')
% figure(3)
% plot(dat(1,:),dat(8,:))
% title('Velocity')
% xlabel('Time [s]')
% ylabel('Velocity[m/s]')
% figure(4)
% plot(dat(1,:),dat(7,:))
% title('Vertical Acceleration')
% xlabel('Time [s]')
% ylabel('Acceleration[m/s^2]')
% figure(5)
% plot(dat(1,:),dat(10,:))
% title('Altitude vs Time')
% xlabel('Time [s]')
% ylabel('Altitude[m]')
% figure(6)
% plot(DragForce(1,:),DragForce(2,:))
% title('Drag Force vs Mach #')
% xlabel('Mach #')
% ylabel('Drag Force [N]')
% figure(7)
% plot(dat(1,:),dat(14,:))
% title('Verical Displacement vs Time')
% xlabel('Time [s]')
% ylabel('Hieght[m]')
```

```
%Drag_Forensic1
function[Cd]=Drag_Forensic1(M)
fudge=0.09;
Cons=.8;
if M<=Cons
  M=Cons;
  Cd=-19.241*M^3+56.037*M^2-52.769*M+16.561+fudge;
%Cd=1.8433*M^3-0.1717*M^2+.0356*M;
elseif M>Cons & M<=1.2
   Cd=-19.241*M^3+56.037*M^2-52.769*M+16.561+fudge;
else
   Cd=-M+1.9736;


End


%m14002
function[Ft]=m14002(tt)% average thrust peak
if tt>=0 & tt<.02
   Ft=49581*tt;
elseif tt>=.02 & tt<.07
   Ft=18961*tt+612.39;
elseif tt>=.07 & tt<.11
   Ft=4363.5*tt+1634.2;
elseif tt>=.11 & tt<.14
   Ft=-4593.7*tt+2619.5;
elseif tt>=.14 & tt<3.53
   Ft=-11.045*tt^2-182.34*tt+1988.6;
elseif tt>=3.53 & tt<3.7
   Ft=-14822*tt^2+105456*tt-186364;
elseif tt>=3.7 & tt<4.43
   Ft=604.45*tt^2-5948.2*tt+14638;
else
   Ft=0;
end
```

```
Ft=.97*Ft;
End


%Atmosphere
function[M,Row,P,T,Y]=Atmosphere(YL,Yr,TL,V)
K=1.4;% Ratio of spec. heat AIR
R=287; %[J/kg*K] Gas constant
tL=TL+273.1; % [K] local temperature
Y=YL+Yr;%[m] Altitude
alpha=-0.00357/(1.8*0.3048);%[change in K or Cels. per meter]
P0=101300;% [Pa]
T0=tL-alpha*YL;
Row=P0/R*((T0+alpha*Y)^(4.26))/(T0^(5.26));% density {kg/m^3]
P=P0*((T0+alpha*Y)/T0)^(5.26);%[pa] Pressure at Altitude
T=P/(Row*R);%[K] Temp at Altitude
M=V/((K*R*T)^(1/2)); %Mach Number
end
```

Distributed Mass Properties Program

```
%Program by Kian Roybal
%Date Created Friday, Sept 20, 2019
%Date Modified Tuesday, October 8, 2019
%Description:
%This program will assist in the design process by allowing a stream-lined
%way to distribute an allowed mass through the distinct sections of the
%rocket. Given a governing diameter is known, and an output
%maximum-allowed-mass from the properties and kinetics calculator are known
%this routine will solve for the thickness that meets it to a safety factor
%stress such that the cross-sectional area satisfies this criteria.
%
%*NOTE* the design method is tentative and is subject to change. Currently
%a change is undergoing, and this file up-to-date does NOT meet the
%description but soon to be updated to function as such.

%Initiate:
clc;clear;close all

%============================%
%===== Rocket sections =====%
```

```
%============================%

%==Material properties===%
%-- Density of material [lb/in.^3]
rho_Al = 0.1;
rho_fiber = .05;

%Governing dimension:
%-- Diameter
D = 8;     %[in.]
R = D/2;   %[in.]

%-- Motor tube [in.]
D_tube = 4;
%this parameter describes the length in which the tube extends from aft end
tube_extended = 4;
L_tube = 12*5+tube_extended;
th_tube = 0.25;
ID_tube = D_tube-th_tube;
[xbar_tube, ybar_tube, zbar_tube, m_tube] = ...
   shell_masscenter(ID_tube,D_tube,L_tube,rho_Al);
Z_cbar_tube = zbar_tube;

%-- Aft end [in.]
L_aft = 12*5;
th_aft = 0.25;
ID_aft = D-th_aft;
[xbar_aft, ybar_aft, zbar_aft, m_aft] = shell_masscenter(ID_aft,D,...
   L_aft,rho_Al);
Z_cbar_aft = zbar_tube+tube_extended;

%-- Center/Ebay [in.]
L_ebay = 12*1;
th_ebay = 0.25;
ID_ebay = D-th_ebay;
[xbar_ebay, ybar_ebay, zbar_ebay, m_ebay] = ...
   shell_masscenter(ID_ebay,D,L_ebay,rho_fiber);
Z_cbar_ebay = Z_cbar_aft+zbar_ebay;

%-- Nosecone [in.]
L_nose = 48;
th_nose = 0.5;
[m_nose,zbar_nose,lala,lsdf,V] = LVH_masscenter(D,th_nose,L_nose,rho_Al);
Z_cbar_nose = Z_cbar_ebay+zbar_nose;

%-- Fincan [in]
L_fincan = 10;
th_fincan = 0.125;
D_fincan = D+th_fincan;
[xbar_fincan, ybar_fincan, zbar_fincan, m_fincan] = ...
```

```
   shell_masscenter(D,D_fincan,L_fincan,rho_Al);
Z_cbar_fincan = Z_cbar_tube + zbar_fincan;

%Fins
th_fin = 0.125;
%This parameter describes distance the point closest to aft end
fins_extended = 2;
%Fin Root Chord
Cr = 8;
%Fin Tip Chord
Ct = 7;
%Fin Semispan
S = 6;
%Midpoint length
Lf = 10.5;


%unitary fin data
[xbar_fin, ybar_fin, zbar_fin, m_fin] = ...
   fin_masscenter(Cr, Ct, S, Lf, th_fin, rho_Al);
%Z_cbar_fins = Z_cbar_tube+fins_extended+zbar;

%Misc. units
n_fins = 4;
theta_seperation = 360/n_fins; %[deg.]
m_fins = m_fin*n_fins;%[lb]

%ZBAR = sum(Z_cbar_i*vol_i)/sum(vol_i);


%Total mass
mass = [m_aft,m_fincan,m_fins,m_tube,m_ebay,m_nose];
mass_Total = sum(mass);%[lb]
V = V*(2.54e1)^3;
fprintf('Resulting Volume of the LV-Haack nosecone is: %1.3e [mm^3]',V);
```

Code Block 1: *Main Routine*

```
function [mass,zbar,outter,inner,vol] = LVH_masscenter(D,th,L,rho)
num = 400;
dx = L/num;
R = D/2;
syms x u

func_radicand = acos(1-2*x/L)-sin(2*acos(1-2*x/L))/2+...
   (2/3)*sin(acos(1-2*x/L))^3;
func = R/sqrt(pi)*sqrt(func_radicand);

OD_int = pi*int(func^2,x,0,L);
```

```
dfunc = diff(func);

dfunc = matlabFunction(dfunc);
func = matlabFunction(func);

len = length(0:dx:L);
[Y,X] = deal(zeros(1,len));
[xx,yy] = deal(zeros(1,len-1));
N = zeros(2,len-1);
for i = 1:len
   X(i) = (i-1)*dx;
   Y(i) = func(X(i));
   if i > 1
      Ni = [dfunc(X(i));-1];
      Nj = th*Ni/norm(Ni);
      N (:,i-1) = Nj;
      xx(i-1) = X(i)+Nj(1,1);
      yy(i-1) = Y(i)+Nj(2,1);
   end
end

%The First least squares fit will be used to solve for the function that
%defines thes the inside radius of the nosecone
%=========================
%----- LEAST SQUARES -----
%--- Sixth order model ---
%=========================
A = ones(len-2,7); flex = xx';
A(:,6) = flex(1:end-1);
bb = yy'; b = bb(1:end-1);
for k = 1:1:len-2
   A(k,1) = xx(k)^6; A(k,2) = xx(k)^5; A(k,3) = xx(k)^4;
   A(k,4) = xx(k)^3; A(k,5) = xx(k)^2;
end
v = (A'*A)\A'*b;
clc;
func_6th = @(xx) v(1)*xx^6+v(2)*xx^5+v(3)*xx^4+v(4)*xx^3+v(5)*xx^2+...
   v(6)*xx+v(7);
xroot = fzero(func_6th,.1,optimset('TolX',1e-8,'Display','off'));
dxx = (L-xroot)/(num-1);
xarray = xroot:dxx:L;
yarray = zeros(1,num);
for i = 1:1:num
   yarray(i) = func_6th(xarray(i));
end

%LV-HAACK function inserted into the mass center definition
%was not integrable by matlab fit the points and integrate the 7th order
%Polynomial fit
```

```
%=========================
%----- LEAST SQUARES -----
%-- Seventh order model --
%=========================
A = ones(len,8); flex_2 = X';
A(:,7) = flex_2;
jj = Y';
for k = 1:1:len
   A(k,1) = X(k)^7; A(k,2) = X(k)^6; A(k,3) = X(k)^5;
   A(k,4) = X(k)^4; A(k,5) = X(k)^3; A(k,6) = X(k)^2;
end
vv = (A'*A)\A'*jj;
func_7th = @(xx) vv(1)*xx^7+vv(2)*xx^6+vv(3)*xx^5+vv(4)*xx^4+vv(5)*xx^3+...
   vv(6)*xx^2+vv(7)*xx+vv(8);
xroot2 = fzero(func_7th,.1,optimset('TolX',1e-8,'Display','off'));
dxx2 = (L-xroot2)/(num);
xarray2 = xroot2:dxx2:L;
yarray2 = zeros(1,num);
for i = 1:1:len
   yarray2(i) = func_7th(xarray2(i));
end
OD_fn = vv(1)*u^7+vv(2)*u^6+vv(3)*u^5+vv(4)*u^4+vv(5)*u^3+...
   vv(6)*u^2+vv(7)*u+vv(8);
OD_Myz = int(u*OD_fn,u,xroot2,L);
OD_mm = int(OD_fn,u,xroot2,L);

ID_fn = v(1)*u^6+v(2)*u^5+v(3)*u^4+v(4)*u^3+v(5)*u^2+...
   v(6)*u+v(7);
ID_int = pi*int(ID_fn^2,u,xroot,L);
ID_Myz = int(u*ID_fn,u,xroot,L);
ID_mm = int(ID_fn,u,xroot,L);

zbar = double((OD_Myz-ID_Myz)/(OD_mm-ID_mm));
zbar = L - zbar;
vol = double(OD_int - ID_int);
mass = rho*vol;
clc;

outter = [X' Y'];
inner = [xarray' yarray'];
end
```

Code Block 2: *LV-Haack Routine*

```
function [xbar, ybar, zbar, m] = fin_masscenter(Cr, Ct, S, Lf, Th, rho)
%DESCRIPTION:
%This function file will return 3D mass center coordinates of a singular
%fin, as well as its mass
%
```

```
%----- output is formatted as follows:
%----- [xbar, ybar, zbar, mass]
%----- Input index:
%----- 1) Cr = Fin Root Chord   :::: dimension: [L]
%----- 2) Ct = Fin Tip Chord    :::: dimension: [L]
%----- 3) S = Fin Semispan      :::: dimension: [L]
%----- 4) Lf = Midpoint length  :::: dimension: [L]
%----- 5) Th = Thickness        :::: dimension: [L]
%----- 6) rho = desnity         :::: dimension: [M/L^3]
%=========================================================================

%Calculated geometry
del = sqrt(Lf^2 - S^2);
l1 = Cr/2 + del - Ct/2;
l2 = Cr/2 + del + Ct/2;

%Composite shape made up of 2 right triangles and a rectangle
%--- Index: [1] Triangle [2] Rectangle [3] Triangle

A1 = 1/2*l1*S;
V1 = A1*Th;
m1 = V1*rho;
xbar1 = 1/3*S;
ybar1 = 2/3*l1;

A2 = (Cr-l1)*S;
V2 = A2*Th;
m2 = V2*rho;
xbar2 = 1/2*S;
ybar2 = l1+1/2*(Cr-l1);

A3 = 1/2*(l2-Cr)*S;
V3 = A3*Th;
m3 = V3*rho;
xbar3 = 2/3*S;
ybar3 = Cr + (1/3)*(l2-Cr);

m = m1 + m2 + m3;

%Compute mass center
xbar = (xbar1*m1 + xbar2*m2 + xbar3*m3)/m;
ybar = (ybar1*m1 + ybar2*m2 + ybar3*m3)/m;
zbar = 0;
end
```

Code Block 3: *Fin Mass Routine*

```
function [xbar, ybar, zbar, m, V] = shell_masscenter(ID, OD, h, rho)
%DESCRIPTION:
```

```
%This function file will return 3D mass center coordinates of a singular
%shell (tube section), as well as its mass.
%
% IMPORTANT NOTE:
% ----- [ for solid cylinder take ID input = 0 ] ----
%
%note: datum of shell is the aft end, with cardinal axes through center
%
%----- output is formatted as follows:
%----- [xbar, ybar, zbar, mass]
%----- Input index:
%----- 1) ID = inner diameter   :::: dimension: [L]
%----- 2) OD = outter diameter  :::: dimension: [L]
%----- 3) h = height of shell   :::: dimension: [L]
%----- 4) rho = desnity         :::: dimension: [M/L^3]
%=========================================================================

%Calculate cross sectional area:
A = pi*1/4*(OD^2 - ID^2);

%Calculate mass properties
V = A*h;
m = V*rho;

%by symmetry and orientation xbar and zbar are centered on origin
xbar = 0;
ybar = 1/2 * h;
zbar = 0;
end
```

Code Block 4: *Shell Mass Routine*

Arduino Pressure Transducer Code

```
/*Author: Kian C Roybal
 *
 * Description:
 * Analog read, the output of a pressure transducer. The pressure transducer is a ratiometric,
 * from 10% to 90% of the power supply voltate. Therefore the analoRead on the pin should give
 * an output that is also a ratio against the maximum specifcation of 1600psi
 *
```

```
*/

//Pin number 14 is the A0 for the arduino uno r3
int dataPin = 14;

//Analog read value corresponding to the reading of the transducer
int val = 0;
int atmospheric = 0;
float atm = 0.0;
float maxPSI = 1600.0;
float maxval = 921.0;
float max1600;
float readPSI;
float gagePressure;

void setup() {
 //Initialize the baud rate of 9600
 Serial.begin(9600);

 //Begin zeroing atmospheric pressure
 delay(100);
 atmospheric = analogRead(dataPin);
 atm = atmospheric;
 delay(100);
 atmospheric = analogRead(dataPin);
 atm = atm + atmospheric;
 delay(100);
 atmospheric = analogRead(dataPin);
```

```
  atm = atm + atmospheric;
  delay(100);
  atmospheric = analogRead(dataPin);
  atm = atm + atmospheric;
  delay(100);
  atmospheric = analogRead(dataPin);
  atm = atm + atmospheric;
  atm = int(atm/5);
  //Atmospheric zeroing complete

  Serial.println("Atmospheric rating: ");
  Serial.print(atm);
  Serial.println("");
  delay(1000);
}

void loop() {
  val = analogRead(dataPin);

  //offset the atmospheric reading to act as a zero
  max1600 = maxval - atm;
  readPSI = val - atm;
  //zeroing complete

  //converts the bits to a gagepressure
  gagePressure = maxPSI *readPSI/max1600;

  //Print data
```

```
  Serial.println("byte reading: ");
  Serial.print(val);
  Serial.println("");
  Serial.println("Pressure reading: ");
  Serial.print(gagePressure);
  Serial.print(" [psi]");
  Serial.println("");
  Serial.println("");
  delay(1);//1000 data per second
}
```

[End of Arduino code: Pressure Transducer]